Influence of Hydrodynamics on the Upper Explosion Limit of Ethene–Air–Nitrogen Mixtures

Jeroen W. Bolk and K. Roel Westerterp
Chemical Reaction Engineering Laboratories, Dept. of Chemical Engineering, University of Twente, 7500 AE Enschede, The Netherlands

A large pilot plant was constructed to study the upper explosion limit of ethene–air–nitrogen mixtures under conditions of flow in a tube. Experiments were performed at pressures of 0.5, 1.0, and 1.5 MPa, gas temperatures between 298 and 573 K, and with ethene concentrations between 20 and 40 vol. %. A cylinder-symmetrical 2-D model developed simulated the experimentally obtained ignition and flame propagation phenomena. The commercial computational fluid dynamics code AEA-CFX 4.1 was used to solve this model, to which reaction kinetics for a scheme of two consecutive reactions were added. The model predicts the experimental explosion points within 0.5 vol. %. The explosion limit is influenced by the gas velocity: it becomes smaller and shifts to higher oxygen concentrations at increasing flow rates. In practice this means that partial oxidation reactions can safely be operated at high oxygen concentrations, provided the gas is kept flowing at high flow rates.

Introduction

In the chemical process industry many processes are dangerous: a typical example is the partial oxidation of ethene to ethene oxide. In a wall-cooled tubular reactor ethene and oxygen are oxidized over a silver-on-alumina catalyst. At specific compositions the mixture of ethene and oxygen can be explosive, and to avoid this the reactor feed is kept under a large excess of ethene. Moreover, a considerable amount of inert material is added to the mixture, usually methane; see Ullmann (1981).

Generally accepted explosion limits cannot be given, because they are affected by pressure, temperature, direction of flame propagation, ignition source, and experimental setup. Explosion limits are usually determined in closed vessels or explosion tubes, with a spark as the ignition source (see, for example, Lewis and Von Elbe, 1961; Zabetakis, 1965; and Lovachev et al., 1973), and the data so obtained are considered to be also valid under industrial operating conditions. The validity of these assumptions has been questioned by Siccama and Westerterp (1993).

Correspondence concerning this article should be addressed to K. R. Westerterp.

For partial oxidation processes the occurrence of sparks in the process equipment as an ignition source is unlikely, because sparks in closed equipment can only be caused by discharges of static electricity. In a partial oxidation process total oxidation always occurs and the water vapors so produced lead to a high electrical conductivity of the gas phase, so that static electricity cannot accumulate. It is more likely that a hot spot acts as an ignition source. Hot spots can be found, for example, in the reactor and heat exchangers. Unfortunately, different ignition sources lead to large differences in ignition characteristics and explosion limits. Coward and Guest (1927) measured ignition of natural-gas–air mixtures by heated metal bars and came to the conclusion that ignition depends on the size and material of the hot spot. Cutler (1974) ignited methane–air mixtures by rapidly heated surfaces; the ignition temperature depended on the heating rate and the size of the hot spot. Detz (1976) also found the ignition of acetylene mixtures depended strongly on the size of the hot spot. Moreover, the gas flow rate affects the heat-transfer rate from the ignition source to the surrounding gas, and therefore the ignition of a combustible gas mixture. In flowing systems igniting an explosive gas mixture is more difficult; see Siccama and Westerterp (1993).

Once the gas is ignited, flame propagation is more difficult in a flowing system than in a stagnant gas due to the increased turbulence and the increased heat and mass transfer from the flame front to the cold, unburnt gas. Lewis and Von Elbe (1961), Watanabe et al. (1983), Leuckel et al. (1989), and Chippett (1993) all concluded that the explosion limit is influenced by the turbulence in the gas mixture.

Zabetakis (1965), Craven and Foster (1966), Gaube et al. (1968), Miller (1969), Fiumara and Cardillo (1976), Crescitelli et al. (1979), and Chippett (1993) have measured the explosion limits of ethene–air–nitrogen mixtures in stagnant systems, so their measurements result in a worst-case analysis, and data from the tests they used for the design of a partial ethene oxidation plant led *a priori* to a highly conservative design with respect to safety.

It is complicated to describe an explosion mathematically, especially in flowing systems at high Reynolds numbers; see, for example, Bird et al. (1960), Wilhelm (1962), Oran and Boris (1981), Borghi (1988), and Libby and Williams (1994). Explosions in flowing systems are characterized by turbulent flow under the strong influence of the chemical reaction. For a complete model, the kinetics and heat effects of all occurring reactions, as well as the physical and chemical properties of all the species involved have to be known as a function of temperature, pressure, and species concentrations. Regretfully, it is unknown which chemical reactions really take place. However, many kinetic schemes have been proposed that use more than 40 different species with at least a hundred different chemical reactions; see, for example, Westbrook et al. (1983) and Warnatz et al. (1994). Furthermore, a model is required to describe the turbulent transport. Many different turbulence models, varying in complexity, are available; see Tennekes and Lumley (1972) and Rodi (1980). Fox (1996) contains a review of the different kinds of approaches applied both in chemical engineering and in combustion science to account for this interaction. Unfortunately, there is no unified approach yet.

Siccama and Westerterp (1993) performed experiments in a small-size tube of 21-mm diameter at low gas velocities, whereas Bolk et al. (1996) used the same tube placed in a larger installation and higher gas flow rates. Explosion limits depended on the flow rate of the gas, an increase of which caused the explosion region to become narrower. In this work the upper explosion limit of ethene–air–nitrogen mixtures with an electrically heated hot wire as the ignition source is studied experimentally under conditions of flow in a larger tube with an internal diameter of 50 mm. A large test installation has been built to perform experiments under conditions similar to those found in a commercial oxidation process. Experiments are performed with varying gas compositions, pressures, temperatures, gas flow rates, hot-spot sizes, and temperatures. Furthermore, a mathematical model has been developed to possibly confirm the experimental data. Chen and Faith (1981) and Siccama and Westerterp (1995) showed that such calculations for combustion phenomena must be extended far into the bulk in order to determine whether the mixture was exploded. The model must at least take into account fluid flow, heat transfer, chemical reaction, and turbulence. We have used the commercial CFD code "AEA-CFX 4.1," which solves a coupled system of mass, momentum, energy, and species equations with the well-known k-ϵ model for turbulence as originally proposed by Jones and Launder (1972).

Experimental Setup

In our specially designed high-pressure laboratory, a large experimental installation for explosion research has been constructed in a concrete bunker. Figure 1 shows the setup. A detailed description of this installation is also given in Bolk et al. (1996).

A stainless-steel tube with an inner diameter of 50 mm and a total length of 3.0 m forms the test section of the installation. It is placed vertically, and the gas flows upwards. The tube consists of three different parts. The first part, an empty tube 2.0 m high, serves to build up and stabilize a turbulent velocity profile. After that the gas passes the ignition source, which is placed in a specially designed part that is discussed later. Finally the gas flows through an empty tube 0.5 m long, in which an ignited gas mixture can propagate. Flame arrestors are placed at both ends of the tube to prevent flame propagation to other parts of the installation. Thermocouples and pressure indicators are placed at several axial positions.

An electrically heated wire of Kanthal A1, an alloy of mainly Fe, Cr, and Al, is used as the ignition source. It is placed either horizontally or vertically. Wires with diameters of 0.6 or 1.0 mm are used. In the vertical position, the wire length is 40 mm. It is connected at both ends to stainless-steel rods of 3.0-mm diameter and placed in the center axis of the tube. In the horizontal position the length of the wire is equal to the tube diameter of 50 mm, and it is also connected at both ends to stainless-steel rods. These rods are now placed outside the tube, so the flow pattern is not disturbed. Both wire orientations are given in Figure 2.

The wires are connected to a computer-controlled power supply from Hewlett-Packard, with a maximum capacity of 200 W for resistance heating. The wire can be observed through a quartz window in the tube wall, for example, with a video camera or a pyrometer. We used a Heimann KT81 pyrometer, which can measure surface temperatures between 1,000 and 1,500 K.

The objective is to measure explosion limits under conditions similar to those in chemical plants, and therefore high gas velocities, pressures, and gas temperatures have to be applied. At such conditions single-pass flow through the installation is not possible, because at the applied high pressures and velocities the gas consumption would become prohibitive. Therefore, recirculation must be applied; to this end a Hofer double-acting recycle piston compressor with a maximum capacity of 30 m^3/h and a maximum operating pressure of 2.5 MPa has been installed. This compressor operates oil-free to prevent oil traces from influencing the explosion characteristics of the gas. The maximum gas flow rate in the 50-mm-inner-diameter tube is 4.0 m/s at all possible pressures.

Ethene, air, and nitrogen are added and controlled by thermal mass flow controllers (Brooks). Heaters are placed in the ethene supply line to counteract the large Joule–Thompson effects during reduction of the pressure from 5.0 MPa in the storage tanks. The gases are mixed before injection into the recycle stream. The ethene concentration is measured on-line with an infrared analyzer, type Servomex Analyzer

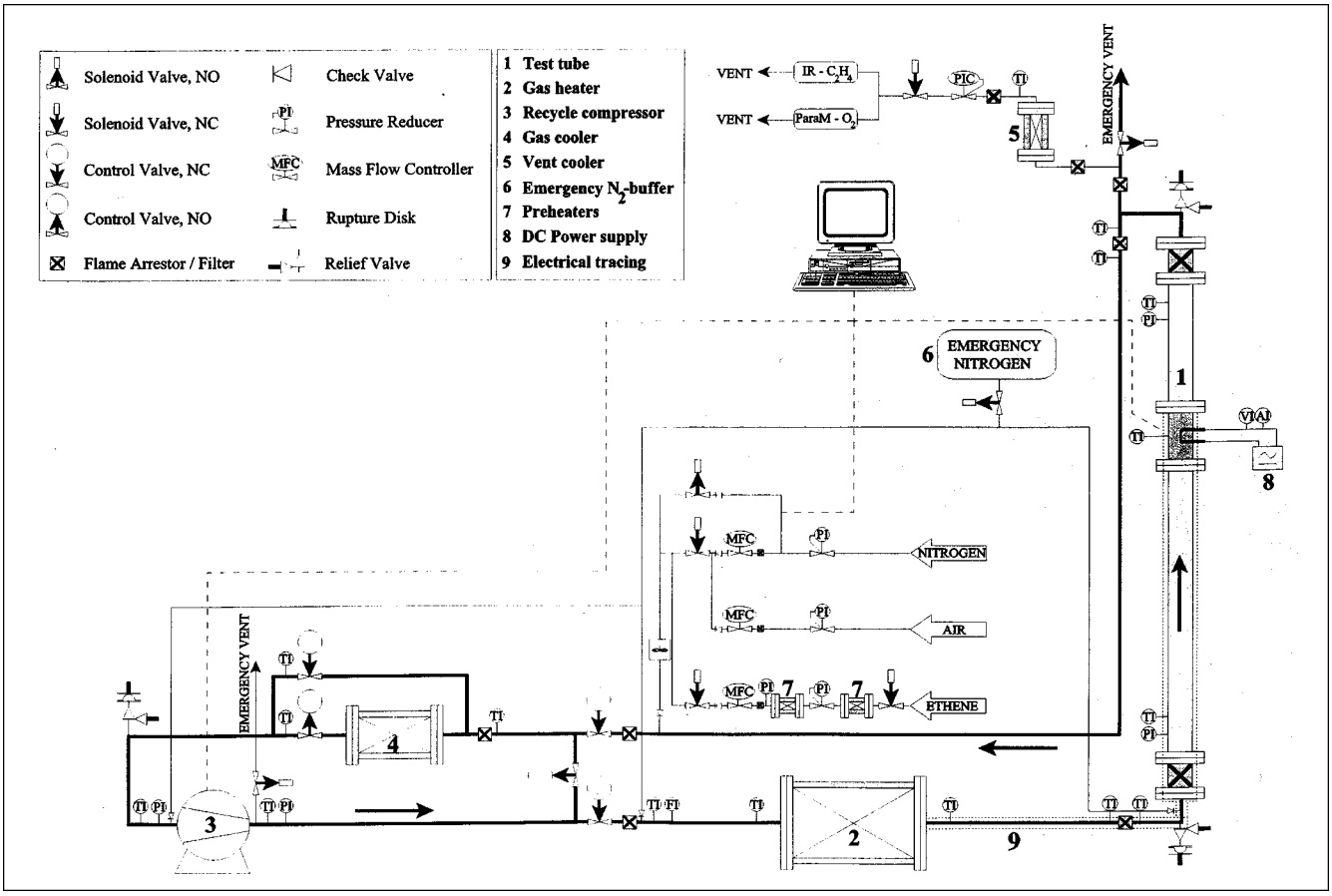

Figure 1. Experimental installation.

Series 1400. The oxygen concentration is measured on-line with a paramagnetic oxygen analyzer, type Servomex Analyzer Series 1100. Both analyzers take their samples from the vent line. The pressure in the installation is maintained by throttling a back-pressure controller in this vent, in which the gas is also cooled to protect both the back-pressure controller and the gas analyzers.

Experiments have been performed up to a maximum temperature of 573 K. The compressor cannot work at such temperatures; therefore, heating and cooling equipment have

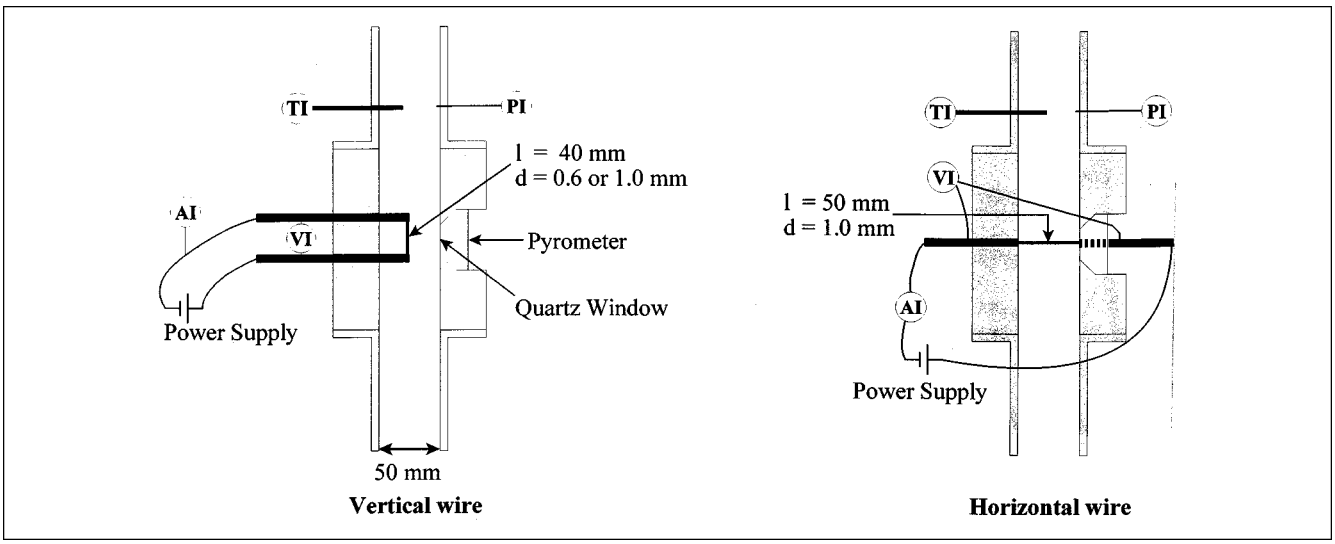

Figure 2. Horizontal and vertical wire orientations.

been installed in the recycle loop. A tube and shell gas–oil heat exchanger (Sinus-Aben), with a maximum capacity of 20 kW, is used to heat the gas with a thermal oil, which is heated electrically and circulated over the shell side. Thermal oil is used to avoid local overheating, which may cause an ignition. The oil temperature is limited to a maximum of 625 K. The tubes from the outlet of the heat exchanger to the test tube, as well as the tube itself, are traced with an electrical heating tape that has a total heating capacity of 5 kW. The gas temperature can be controlled by the power supply to the tracing. Since the maximum inlet temperature of the compressor is limited to 425 K, the recycle gas is cooled before the compressor in a gas cooler with a cooling capacity of about 20 kW. The inlet temperature of the compressor is controlled automatically by sending the recycle gas through a bypass located over the cooler.

The gas velocity in the test tube is measured with a Höntsch propeller measuring probe, placed in the recycle line and controlled by control valves in a bypass of the compressor. These control valves also give resistance to the flow to muffle the pulsations of the piston compressor.

Much attention has been paid to safety. The installation is placed in a concrete bunker and fully computer controlled. At crucial places in the recycle line, additional flame arrestors have been placed. Furthermore, thermocouples and pressure indicators in various places are used to determine the temperatures and pressures in the system every 8 s. If a measured value indicates a dangerous situation, the experiment is terminated automatically and the system purged with nitrogen from an emergency buffer. Relief valves, which discharge at pressures exceeding 3.0 MPa, are placed at both ends of the explosion tube and at the inlet of the compressor. Rupture disks protect the installation for pressures exceeding 4.0 MPa. The gas escaping from these devices is vented outside the bunker to the open air. Combustible gas detectors connected to a Servomex control unit are placed at strategic points in the bunker, to monitor leakage of combustible gas. If a leak is observed, the experiment is stopped and the installation is flushed with nitrogen.

Experimental Procedure

At the beginning of an experiment the compressor is started, the gas is recycled at maximum velocity through the installation, and any oxygen is removed by flushing the entire installation with nitrogen. After that ethene and air are added to the recycle flow via calibrated Brooks mass flow controllers. Nitrogen is used to balance the gas mixture. This sequence is chosen to avoid gas compositions that may be explosive in the recycle. In most experiments the ethene concentration is kept constant at 25 vol. %. When the concentration has stabilized within 1.0 vol. % of the desired composition, oxygen is added and controlled within 0.1 vol. % of its set point. For safety reasons, the ethene and oxygen concentrations are set at the minimum pressure in the installation. Pressure has a large influence on the explosion limits, and a pressure increase enlarges the explosion region; see Zabetakis (1965), Craven and Foster (1966), Gaube et al. (1968), Miller (1969), Fiumara and Cardillo (1976), Crescitelli et al. (1979) and Siccama and Westerterp (1993).

Once the gas composition has been set, the pressure is increased by throttling the electronic back-pressure controller in the vent. The maximum operating pressure is 1.5 MPa. The gas velocity is set by the control valves in the recycle, and after that, if necessary, the gas heater, electrically heated tracing, and cooler are put into use.

Because of the size of the equipment, reaching steady-state conditions normally takes 30 to 60 min. After that, during a 30-s period, the wire is heated electrically, and the pressure and temperature in the tube, the power supply to the wire, and the temperature of the wire via the pyrometer are measured at a rate of about 100 Hz. The gas mixture is considered ignited when the pressure suddenly rose by more than 0.05 MPa or the temperature by at least 200 K. The power supply to the wire is then switched off and all valves set immediately in their fail-safe position. Simultaneously the installation is flushed with nitrogen. Uncontrolled flame propagation to other parts of the installation can be avoided in this way, and the formation of soot within the recycle system is minimized.

If the gas mixture ignites, a similar experiment is performed at other initial conditions of pressure, temperature, or gas velocity. If no ignition is observed, the experiment is repeated with an increased power supply to the wire or an increased oxygen concentration. Thus, the experiments are performed at constant pressure, temperature, and gas velocity as a function of the power supply to the wire and the oxygen concentration.

Experimental Results

Explosion points are measured at different experimental conditions (Table 1). At constant pressure, temperature, and gas velocity the power supply to the wire and the oxygen concentration are varied to construct a typical explosion diagram, as given in Figure 3. Generally, six to eight experiments have been carried out at different power-supply rates to the wire and oxygen concentrations in the gas mixture, whereas the ignition of a local reaction around the wire or a reaction propagating through the tube have been measured and a figure similar to Figure 3 constructed. Points 1 to 5 indicate five different conditions for which the temperature profiles have been calculated by the model, as is discussed later. In this diagram three different regions can be distinguished: the regions of negligible reaction, local reaction, and explosion. A reaction does not occur when the power-supply rate to the wire, and thus the temperature of the wire, is too low. Increasing the power supply to some specific value initiates combustion. This minimum power-supply rate is independent of the oxygen concentration and can be represented by a horizontal line in the explosion diagram of Figure 3.

Table 1. Experimental Operating Conditions

Pressure	0.5, 1.0 and 1.5 MPa
Temperature	298, 423, 473, 498, 523 and 573 K
Gas velocity	0.25 to 4.0 m/s
Composition	
Ethene	20, 25, 30 and 40 vol. %
Oxygen	7.5 to 15.0 vol. %
Nitrogen	Variable

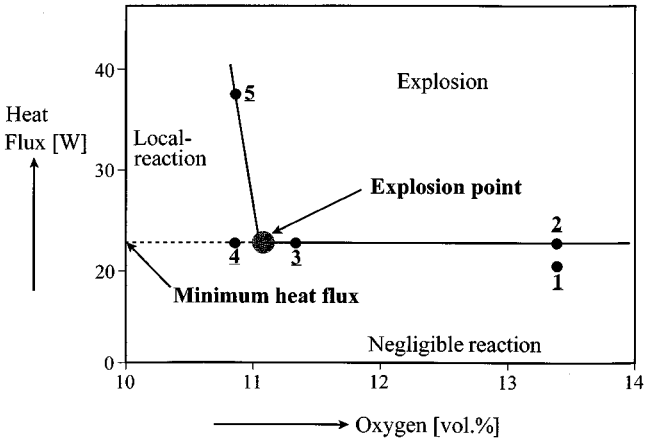

Figure 3. Explosion diagram; numbers 1 to 5 refer to Figures 11a to 11e.

Above this value either a local reaction around the heated wire or an explosion will occur, depending on the oxygen concentration. The boundary between these two regions can be given by an almost vertical line with a negative slope, as in Figure 3. The point of intersection between the boundary lines of local reaction, explosion, and of the minimum power supply has been designated the explosion point (see Siccama and Westerterp, 1993).

The temperature of the wire depends on the power supply to the wire and the heat transfer rate from the wire to the flowing gas. The wire requires a minimum power supply, and thus a minimum temperature, to ignite the gas mixture. Unfortunately, the temperature of the wire could not be measured because it was below the 1,000 K detection limit of the pyrometer under all conditions. The minimum power-supply rates as a function of the Reynolds number (Re) are shown in Figure 4; for horizontal wires they are significantly higher than for vertical wires. The Reynolds number is based on the tube diameter, and the density and viscosity are taken for air at the conditions in the tube before the ignition wire. Heat transfer from horizontal wires is better than for vertical wires

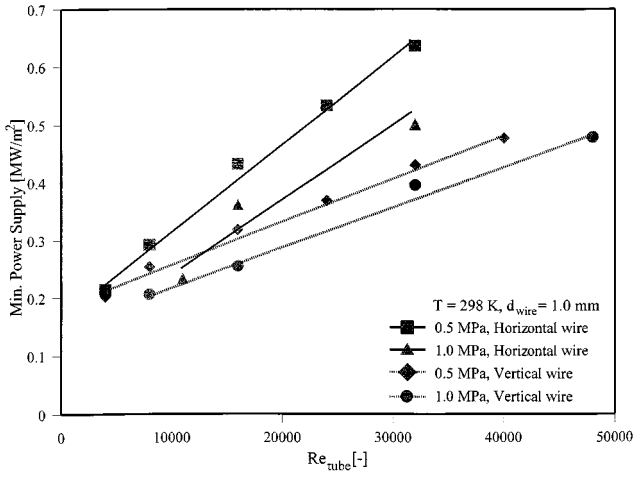

Figure 4. Minimum power supply at ignition, expressed in MW/m^2 wire surface.

(see, e.g., Ulsamer, 1932; Hilpert, 1933; Beek and Muttzall, 1975; Perry et al., 1984). This means that, at equal Reynolds numbers and power supply rates, the temperature of a horizontal wire is lower, thus ignition with horizontal wires is more difficult than with vertical ones. The estimated temperature of the wire at ignition is around 1,000 K.

Once the gas has been ignited, the reaction can propagate through the tube, depending on the oxygen concentration. This is only possible if the heat generated by the combustion reactions is larger than the heat removed by the turbulence from the reaction zone to the unburnt gas (see Semenoff, 1928; Frank-Kamanetskii, 1969). At sufficiently high power supplies, but at low oxygen concentrations, the heat production rate of the combustion reactions is not high enough and only a local reaction occurs around the wire over a certain volume: the heat production rate is balanced by the heat removal rate and the reaction remains localized around the wire. Thermocouples close to the wire display a temperature significantly higher than when no reaction takes place. A decrease in the oxygen concentration and the formation of soot are other indications of a reaction taking place. No increase in temperature or pressure is observed in the tube. An increase in the oxygen concentration during a subsequent experiment causes the local reaction to suddenly change into an explosion, because the heat production rate increases to a level where it is no longer balanced by the heat removal. This can be observed by a very fast and large temperature increase, and is usually accompanied by a pressure increase in the tube.

To summarize, a minimum power supply rate to the wire is required for gas to ignite. Once the gas is ignited, propagation is only possible for sufficiently high oxygen concentrations. Thus the explosion point indicates the minimum power supply and the minimum critical oxygen concentration where flame propagation becomes possible. This explosion point can be experimentally determined for different gas velocities, pressures, temperatures, gas compositions, and wire sizes and orientations.

Explosion points for different wires

Vertical wires with diameters of 0.6 and 1.0 mm and horizontal wires with a diameter of 1.0 mm have been used to ignite the gas at temperatures of 298 K and pressures of 0.5 and 1.0 MPa. Results are given in Figure 5 as the critical oxygen concentration in the explosion point as a function of the Reynolds number in the tube. In all cases the power supply to the ignition wire is just above its minimum value (see Figure 3).

Increasing the gas flow improves the heat-removal processes. To counterbalance this effect, the oxidation reaction must produce more heat to maintain a reaction. Because of the excess ethene this means the oxygen concentration has to be increased to induce an explosion at higher gas flow rates.

The critical oxygen concentration does not change much for the different wire diameters and orientations: for horizontal wires it is about 0.5% lower than for vertical wires. The dependence on the gas flow rate is the same for both wire orientations.

Obstacles in the tube disturb the gas flow, because they create vortices that increase the turbulence. Horizontal wires

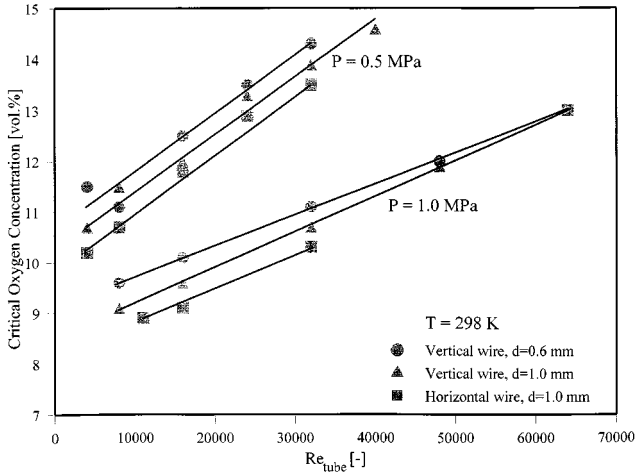

Figure 5. Critical oxygen concentrations in the explosion point with different wires as ignition source.

exert only a slight disturbance in the gas flow, because the connecting rods are placed outside the tube. Vertical wires are kept in the middle of the tube by connecting rods with a diameter of 3.0 mm, as shown in Figure 2; these rods disturb the gas flow and slightly increase the heat removal rate. To counterbalance this effect the combustion reaction must generate more heat, so the critical oxygen concentration shifts to higher values for vertical wires.

Experiments at different pressures

The critical oxygen concentration at pressures of 0.5, 1.0 and 1.5 MPa is plotted as a function of the Reynolds number in Figure 6. In all cases a vertical wire with a diameter of 1.0 mm has been used.

An increase in the pressure causes the critical oxygen concentration to decrease, thus enlarging the explosion region. This was also observed with experiments in quiescent mixtures (see, e.g., Zabetakis, 1965; Craven and Foster, 1966; Gaube et al., 1968; Miller, 1969; Fiumara and Cardillo, 1976; and Crescitelli et al., 1979). A clear explanation for this effect has not been given. A pressure increase may increase the reaction rate, because the reactant concentrations are increased, as is the heat production rate. However, the lower explosion limit remains almost constant with increasing pressure. Probably, the reaction mechanisms are different at the upper and the lower limits of the explosion region.

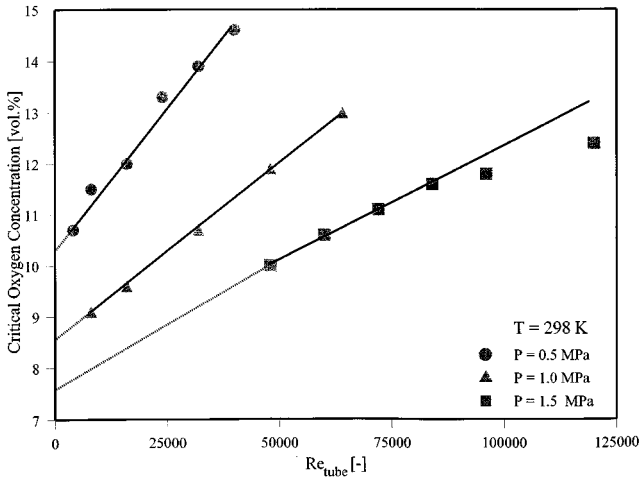

Figure 6. Influence of pressure on critical oxygen concentrations in the explosion point; interrupted lines are extrapolated.

An increase in the gas velocity has the same effect independent of the system pressure: the explosion region becomes smaller when the gas flows. Siccama and Westerterp (1993) and Bolk et al. (1996), who showed explosion experiments in quiescent mixtures, give worst-case results, because the experiments resulted in the lowest critical oxygen concentration at the explosion point.

Explosion limits in stagnant gases can be found by extrapolation in Figure 6 to a zero Reynolds number. The values obtained can be compared with data on explosion limits in stagnant ethene–air–nitrogen mixtures at room temperature and different pressures that can be found in the literature (see Table 2). Our extrapolations of the critical oxygen concentrations are consistent with the experiments performed in quiescent mixtures.

Experiments at different temperatures

Typical operating temperatures in ethene oxidation reactor systems are around 500–550 K. Experiments in quiescent mixtures showed that the explosion region is enlarged with increasing temperature (Zabetakis, 1965; Craven and Foster, 1966; Gaube et al., 1968; Miller, 1969; Fiumara and Cardillo, 1976; and Crescitelli et al., 1979). Experiments at gas temperatures up to 573 K are shown in Figure 7 for pressures of 0.5, 1.0 and 1.5 MPa, respectively. In all situations the Reynolds number is kept constant at the different temperatures.

Table 2. Critical Oxygen Concentrations at $Re \rightarrow 0$ vs. Experimental Results in Quiescent Mixtures*

Press. [MPa]	Crit. Oxygen Conc. [Vol. %]	Reference
0.1	15.0	Gaube et al. (1968)
	14.0	Craven and Foster (1966)
	12.5	Zabetakis et al. (1965)
	15.4	Hashiguchi et al. (1966)
0.3	11.5	Craven and Foster (1966)
0.5	10.4	This work
	11.6	Hashiguchi et al. (1966)
0.7	10.0	Gaube et al. (1968)
0.9	8.8	Craven and Foster (1966)
1.0	8.6	This work
	8.4	Fiumara and Cardillo (1976)
	9.5	Hashiguchi et al. (1966)
1.5	7.7	This work
	7.55	Fiumara and Cardillo (1976)
2.0	8.1	Hashiguchi et al. (1966)
3.0	6.3	Fiumara and Cardillo (1976)
	6.7	Hashiguchi et al. (1966)

*Temperature is 298 K.

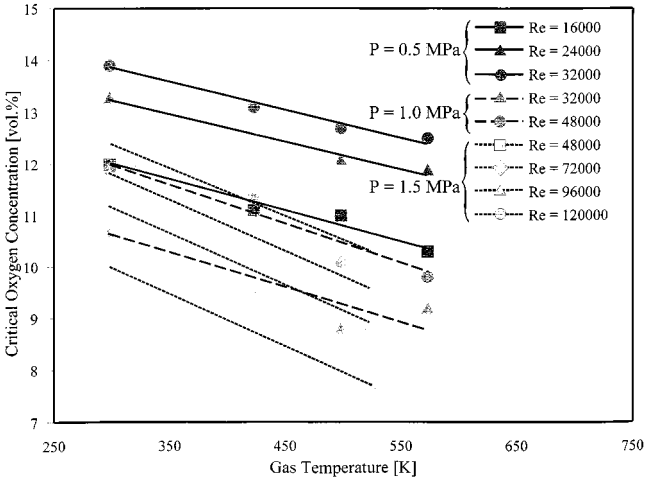

Figure 7. Influence of gas temperature on the critical oxygen concentrations in the explosion point at $P = 0.5$, 1.0 and 1.5 MPa.

An increase in gas temperature causes a decrease in the oxygen concentration at the explosion point, and the explosion region enlarges. Burgess and Wheeler (1911) produced a relation to estimate the lower explosion limit. The product of the fraction combustible X times the heat of combustion, ΔH_{comb}, of the combustible gas is constant:

$$X_{O_2}\Delta H_{comb} = \text{constant}. \tag{1}$$

Equation 1 can be modified to include the influence of the temperature. The heat release per mole of mixture at the explosion limit must be so large that after adiabatic combustion the products have a certain temperature T_{flame}:

$$cX_{O_2}(T)\Delta H_{comb} = \rho C_p(T_{flame} - T). \tag{2}$$

Equation 2 implies that the percentage of combustible at the lower limit varies linearly with temperature. This modification of Eq. 1 is called the modified Burgess and Wheeler equation or the rule of the constant flame temperature, which is given in Eq. 3:

$$\frac{X_{O_2}(T)}{X_{O_2}(T_{room})} = 1 - \frac{(T - T_{room})}{(T_{flame} - T_{room})}. \tag{3}$$

Equation 3 has been proven by, for example, White (1925) and Hustad and Sønju (1988), to be valid for different gas mixtures at the lower explosion limit. Zabetakis (1965) found it was also valid for the upper explosion limit. For ethene mixtures he derived a flame temperature of about 1,500 K. Statistical analysis of our data by a least-squares method and extrapolation to zero oxygen concentration results in a flame temperature of approximately 1,750 K for the experiments performed at 0.5 MPa, 1,500 K at 1.0 MPa, and 1,250 K at 1.5 MPa. Bolk et al. (1996) did similar tests in a smaller 21-mm tube and found a flame temperature of around 1,500 K at a pressure of 0.5 MPa.

Experiments at 573 K and 1.0 MPa and at 523 K and 1.5 MPa were difficult to evaluate. The boundaries between the different regimes shown in Figure 3 became less sharp, so there is a transition region between local reaction and explosion. This is probably caused by an instability of ethene at these high temperatures and pressures and preoxidation taking place before ignition (see, e.g., Craven and Foster, 1966; and Crescitelli et al., 1979).

Experiments at different ethene concentrations

Most experiments have been carried out at an ethene concentration of 25.0 vol. %. Experimenters have used ethene concentrations between 20 and 40 vol. % to investigate its effect on the explosion limit. This is still a large excess compared to the approximately 10 vol. % of oxygen. An increase in the ethene concentration reduces the nitrogen content. Experiments have been performed at pressures of 1.0 and 1.5 MPa and at gas temperatures of 298 and 498 K.

From these experiments, we observe a slight increase in the critical oxygen concentration with increasing ethene concentrations, which means the explosion region becomes smaller. Increasing the ethene concentration raises the heat capacity of the mixture. Lewis and Von Elbe (1961), Zabetakis (1965), Craven and Foster (1966), and Crescitelli et al. (1979) showed an inert with a large capacity to absorb heat is the best material to avoid explosions. For example, they compared the inertness of nitrogen with carbon dioxide and concluded that carbon dioxide is better because of its higher heat capacity. The heat capacity of ethene is larger than that of nitrogen, so the total heat capacity of the mixture becomes larger for higher ethene concentrations and the explosion region decreases, shifting to higher critical oxygen concentrations.

In Figure 8 the critical oxygen concentration divided by the heat capacity of the gas mixture has been plotted as a function of the ethene concentration. Now the critical oxygen concentration is independent of the ethene concentration. Thus, the increase in critical oxygen concentration at higher

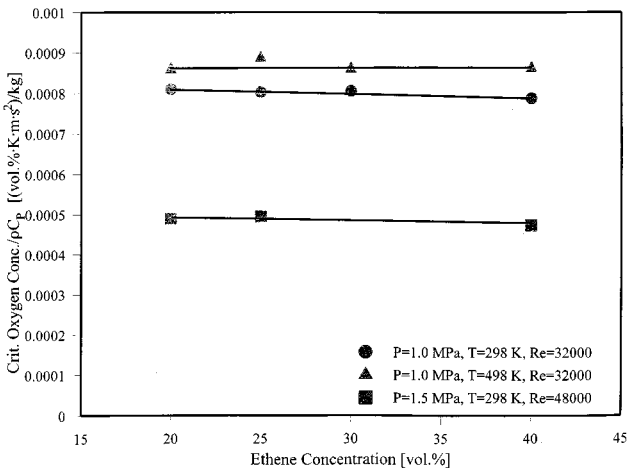

Figure 8. Critical oxygen concentrations in the explosion point divided by the volumetric heat capacity of the gas mixture vs. the ethene concentration.

ethene concentrations is probably caused by an increase in the heat capacity of the gas mixture.

Mathematical Model

Basic equations

The mathematical model consists of the fundamental equations of change describing the conservation of mass, momentum, and energy. With computers solving these equations, these conservations are only possible in a laminar situation or at low Reynolds numbers and for simple geometries (see, e.g., Oran and Boris, 1981; and Fox, 1966). In a more complicated turbulent flow the equations cannot be solved directly, so they are averaged to get equations for the mean and the mean square value of randomly fluctuating variables (see Bird et al., 1960; and Libby and Williams, 1994). We will use turbulence models, which solve transport equations for the Favre-averaged quantities. The time-smoothed equations with Reynolds stresses and fluxes are given below for when the turbulent fluctuations of the density are assumed to be very small and therefore can be disregarded:

Continuity equation:

$$\frac{\partial \rho}{\partial t} + (\nabla \cdot \rho \bar{u}) = 0. \tag{4}$$

Momentum equation:

$$\frac{\partial (\rho \bar{u})}{\partial t} + (\nabla \cdot \rho \bar{u}\bar{u}) = -(\nabla \cdot \bar{p})\delta_{ij} - (\nabla \cdot \overline{\tau_L}) - (\nabla \cdot \overline{\tau_T}) + \rho g$$

$$\bar{\tau}_L = -\mu_L\left(\nabla \bar{u} + (\nabla \bar{u})^T\right) + \left(\frac{2}{3}\mu_L - \kappa\right)(\nabla \cdot \bar{u})\delta_{ij}. \tag{5}$$

Energy equation:

$$\frac{\partial (\rho \bar{h})}{\partial t} + (\nabla \cdot \rho \bar{u}\bar{h}) = \frac{\partial p}{\partial t} - (\nabla \cdot \overline{q_L}) - (\nabla \cdot \overline{q_T}) + \rho u g + \overline{Q_R} + Q'_R$$

$$\overline{q_L} = -\frac{\lambda}{C_P}\nabla \bar{h} + \left(\frac{\lambda}{C_P} - \rho D\right) \cdot \bar{h}_s \nabla \bar{Y}_s. \tag{6}$$

Continuity equation for species mass fractions:

$$\frac{\partial (\rho \bar{Y}_s)}{\partial t} + (\nabla \cdot \rho \bar{u} \bar{Y}_s) = -(\nabla \cdot \overline{J_{s,L}}) - (\nabla \cdot \overline{J_{s,T}}) + M(\bar{r}_s + r'_s)$$

$$J_{s,L} = -\rho D \nabla \bar{Y}_s \tag{7}$$

The following assumptions have been made:

- The flow is compressible and the pressure work term is ignored in Eq. 6.
- The energy transfer due to the work done by body forces, normally denoted by $\rho u g$, can be neglected when compared to the other terms in Eq. 6.
- When the Lewis number (Le) is set to one, the rate of energy transport equals the rate of mass transport, and the second term of the laminar heat flux vanishes.
- The overpressure is very small compared to the initial pressure and its contribution to the density can be ignored. So, pressure waves have been ignored and the speed of sound is infinite. These assumptions are valid for flows at low Mach numbers (Ma), usually $Ma < 0.3$; this is true for our type of flow, in which only small pressure increases have been measured experimentally, typically a maximum pressure increase of 5% of the initial system pressure.
- At low Mach numbers the contribution of the kinetic energy term in the total enthalpy can be neglected and the viscous dissipation is negligible.
- Dufour terms (transfer of energy due to a concentration gradient) have been neglected in Eq. 6.
- In Eq. 7 the influence of diffusion due to temperature gradients (Soret effect) and due to pressure gradients have been neglected.
- The ideal gas law has been used to relate the pressure and the density:

$$\rho = \frac{P_0}{RT\sum_{s=1}^{ns}\frac{Y_s}{M_s}}. \tag{8}$$

- Due to the nonlinear convective term in the nonaveraged equations, additional terms arise in the averaged equations. These terms reflect the fact that convective transport due to turbulent velocity fluctuations will act to enhance mixing over and above that caused by thermal fluctuations at the molecular level. At high Reynolds numbers, turbulent velocity fluctuations occur over a length and time scale much larger than the free path of the thermal fluctuations; hence, the turbulent fluxes are much larger than the molecular fluxes. Furthermore, only the first-order reaction of the chemical reaction term has the same form in the time-smoothed equation as in the original equation. Reactions not of the first order under time-smoothing generate the additional terms r'_s and Q'_R (see Bird et al., 1960). We assume that the size of these fluctuations is small compared to the mean reaction rate, and that they can be neglected.

Equations 4 to 7 have to be solved by providing models for the computation of the turbulent momentum stresses and turbulent energy and mass fluxes. We have used the well-known and well-tested k-ϵ model, because it has been used successfully in many applications in which homogeneous turbulence is present.

Grid and discretization

The equations have been solved by the ''finite volume method,'' which means that the flow domain is divided into a finite number of cells and that the equations are discretized. All variables are located in the cell centers, whereas the velocity components at the cell faces are calculated by interpolation. This is called a *nonstaggered grid*. If the connecting rods of the vertical wire are neglected, the test tube and the wire are rotation-symmetrical, so that a two-dimensional rectangular grid can be used, in our case, with, in the axial direction, 500 grid cells that vary in size from 0.5 mm to 1.5 mm, and in the radial direction, 50 cells that vary from 0.06 mm to 0.5 mm. The smallest cells have been located close to

the wire, because the largest temperature gradients occur in that region (see Figure 9). The wire has been placed as an obstacle in the axis 10 mm behind the inlet. In the radial direction the size is equal to the radius of the wire, which is 0.3 mm in the 21-mm tube and 0.5 mm in the 50-mm tube; it contains five equally sized grid cells. In the axial direction the length is equal to the 40.0-mm long wire, and 80 grid cells of 0.5 mm have been used.

Different differencing schemes have been used to discretize the equations. Hybrid differencing was applied for all variables except pressure. This scheme uses central differencing in regions of low gas velocities, and upwind differencing in regions of high gas velocity. Numerical diffusion has been reduced, and the scheme is first-order accurate. Pressure was calculated using a central differencing scheme, which is always second-order accurate.

The equations have been solved time dependently, using a fully implicit first-order Euler backward-difference, time-stepping procedure. Because of the immutable properties of the set of equations, the flow equations have been decoupled from the enthalpy and mass-fraction equations. Typical time steps for the flow are between 10^{-1} and 10^{-3} s, whereas for the enthalpy and mass-fraction equations false time steps have been used up to a minimum of 10^{-15} s. Calculations were executed until steady state was reached. Slow convergence was observed as soon as the gas started to react, and the flame front propagated through the tube. The final result is that all oxygen has been consumed completely, at least downstream of the wire.

Boundary conditions

Also in Figure 9, the boundary conditions are given for the flow domain. Dirichlet boundary conditions were used at the inlet of the tube. In an empty pipe without wire, a rough grid of 100 20.0-mm cells with the same grid distribution in the radial and axial directions, a fully developed turbulent flow was calculated. The values of the radial velocity distribution

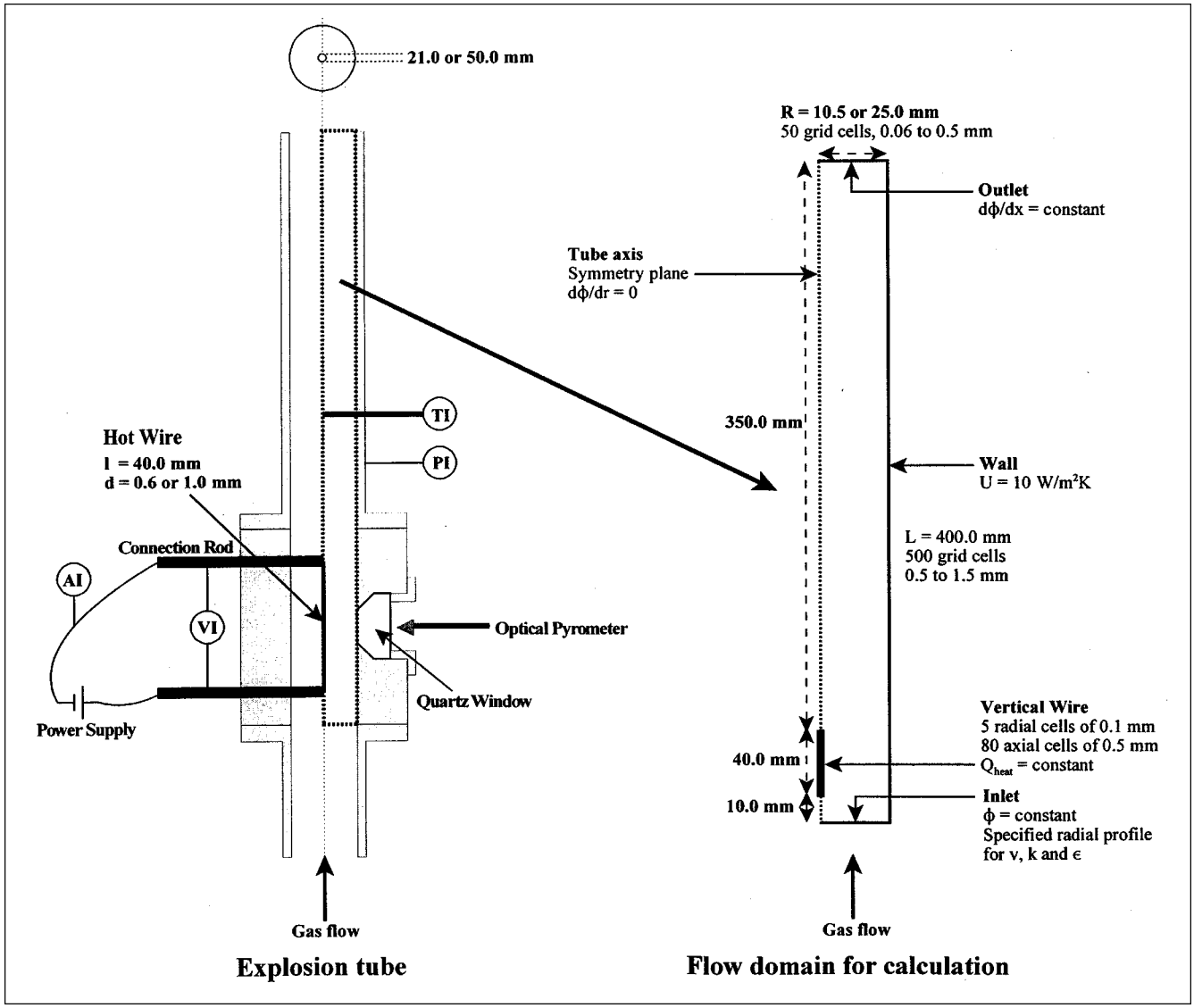

Figure 9. Domain for the calculation.

and of k and ϵ at the outflow of such a tube were used as the inlet boundary condition for the calculation of the reacting flow. Neumann boundary conditions were used at the outlet of the flow domain. All variables were given zero gradients, except the velocity, which was given a constant gradient to maintain conservation of mass. The axis of the tube can be seen as a symmetry line, and here all variables have zero gradients. A no-slip boundary condition was used on the solid surfaces: the velocity equals zero at the tube wall and on the wire surface, and logarithmic wall functions were used near the walls. The tube wall is considered to be nonadiabatic, and the heat transfer from the inside wall of the pipe to the environment is represented by a uniform overall heat-transfer coefficient U of 10.0 $W \cdot m^2 \cdot K^{-1}$, the value of which has hardly any influence on the outcome of our calculations.

The wire can be seen as a solid obstacle in the flow with the physical properties of Kanthal A1, an alloy of mainly Fe, Cr, and Al. The temperature of the wire was calculated by specifying a constant heat flux to the wire instead of a fixed temperature, just as in the experiments. Hence, the following enthalpy equation has been solved for the wire:

$$\frac{\partial(\rho_{\text{sol.}} H)}{\partial t} = \left(\nabla \cdot \frac{\lambda_{\text{sol.}}}{C_{p,\text{sol.}}} \nabla H \right). \tag{9}$$

Continuity of temperature and heat flux was assumed at the interface between the wire and the fluid; thus the heat flux to the gas could be calculated.

Physical properties

The ideal gas law was used to calculate the density (see Eq. 8). In the combustion process temperatures may vary between 298 and more than 2,000 K, and because the temperature is deduced from the local enthalpy and the total heat capacity, the correct calculation of the specific heat of the gas mixture is essential. Assuming that the specific heat is constant may influence the results dramatically (Merzhanov and Averson, 1971; Rota et al., 1991). The specific heat of the mixture was taken as the weighted average of the values of the components, whereas the specific heat of the individual components was taken as a fourth-order polynomial function of the temperature.

The turbulent transport properties—that is, the effective viscosity, the effective thermal conductivity, and the effective diffusion coefficients—consist of the total molecular and turbulent contributions. The turbulent viscosity as calculated by the k-ϵ model depends on the flow and the physics of the system. The turbulent conductivity and turbulent diffusion coefficients were then calculated using a turbulent Prandtl (Pr) or Schmidt (Sc) number of 0.9. The gas viscosity was set to 1.75×10^{-5} Pa·s, the thermal conductivity to 2.52×10^{-2} W/m·K, and all the species diffusion coefficients to 1.7×10^{-5} m^2/s. Small inaccuracies in these values do not alter the results, because the molecular contributions are at least 10^2–10^3 times smaller than the turbulent ones (see Bird et al., 1960).

The physical properties of the wire were considered to be constant. Kanthal A1 has a density of 7,100 kg/m^3, a specific heat of 460 J/kg·K, and a thermal conductivity of 25.0 W/m·K.

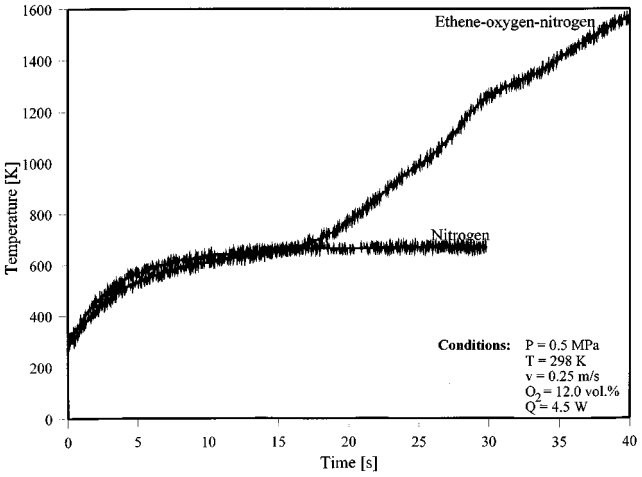

Figure 10. Course in time of the platinum wire temperature during an explosion.

Kinetics Applied in the Model

The surface temperature of the ignition wire was measured via an optical pyrometer. Unfortunately, the temperature of the wire at the ignition point is still below 1,000 K, the lower detection limit of the pyrometer. Therefore, for wires made of pure nickel or platinum and of 0.5-mm diameter, the change in electrical resistance was measured during an experiment. The temperature was determined from those data. A typical temperature progression for a platinum wire as a function of time during its heating period is given in Figure 10. In this figure two lines have been plotted. The wire temperature was calculated at a given pressure, gas feed temperature, and velocity for a combustible mixture of ethene–oxygen–nitrogen and for only nitrogen flowing through the tube. In the case of nitrogen, the temperature of the wire reaches a constant value of around 650–700 K, where the heat production rate is balanced by the heat removal rate. In the case of an ethene–oxygen–nitrogen mixture, a completely different temperature progression was observed. The temperature does not reach a constant value, but continuously increases to more than 1,500 K; this is probably because of the heterogeneous reactions taking place on the surface of the wire (see, e.g., Cutler, 1974; Williams et al., 1991; Veser and Schmidt, 1996). These reactions release heat, causing the temperature to rise to the point where an explosion starts. The experiment was terminated after the explosion.

Laurendeau and Caron (1982) observed similar temperature progressions for methane–air mixtures ignited with a tungsten strip. Cho and Law (1986) measured the temperatures of platinum wires, igniting different fuel–oxygen–nitrogen mixtures, and observed a jump in the wire temperature when the surface reactions started. For ethene–air mixtures at the lower explosion limit, they measured an ignition temperature of 500°C.

Once these heterogeneous reactions were started, the temperature of the wire increased, and, eventually, homogeneous reactions occurred in the gas phase; these reactions remained localized around the wire or propagated through the entire tube, depending on the oxygen concentration. In the propa-

gation case, a sudden increase in temperature and pressure was observed, after which the experiment was terminated. Propagation is only possible if the heat generated by the gas-phase reactions is larger than the heat removed from the reaction zone to the unburnt gas, which is influenced by the turbulence (see Semenoff, 1928; Gray and Lee, 1967; Frank-Kamenetskii, 1969).

Thus, for a complete kinetic model it is necessary to describe the heterogeneous and the homogeneous reactions as well as the coupling between them. However, it is not known which heterogeneous reactions take place and, furthermore, the coupling between the heterogeneous and homogeneous reactions is very complex and not yet fully understood (see, e.g., Veser and Schmidt, 1996). Therefore, in the model the heterogeneous reactions were neglected and only the homogeneous reactions were taken into account.

A detailed description of the homogeneous gas-phase reactions in case of ethene combustion requires a chemical scheme consisting of at least 40 different components and more than 100 reaction steps, according to, for example, Oran and Boris (1981), Westbrook et al. (1983), and Warnatz et al. (1994). These schemes have been tested only near stoichiometric conditions, whereas we used a large excess of ethene. Moreover, incorporation of such kinetic schemes into Eqs. 4 to 9 makes the model far too large to solve, in view of the present state of computing power. In our case, the model should give the critical oxygen concentrations at which propagation of the reaction through the tube is possible. For this purpose, calculation of the correct heat production rate is important, because propagation is only possible when the heat production rate is larger than the heat removal rate. Simple chemical schemes can be used for this, and these schemes have been given in the literature (see, e.g., Westbrook and Dryer, 1981; Birkan and Law, 1987; Singh and Jachimowski, 1994). Complete schemes have been used to lump the kinetic parameters of the simple schemes, and as a result, both schemes yield about the same adiabatic flame temperature. This is only the case if both schemes predict the same heat production rate.

Initially, a one-step total combustion of ethene was incorporated into the model. We applied the simplified scheme with kinetic parameters given by Westbrook and Dryer (1981), which are often used for this purpose:

$$C_2H_4 + 3O_2 \rightarrow 2CO_2 + 2H_2O. \tag{10}$$

This model overestimates the heat production rate, so that the propagation of the reaction front through the gas mixture occurs at critical oxygen concentrations considerably lower than those found in our experiments. Therefore, a two-step scheme was eventually used, which predicted the real heat production rate more accurately:

$$\begin{aligned} C_2H_4 + 2O_2 &\xrightarrow{r_1} 2CO + 2H_2O \\ 2CO + O_2 &\underset{r_3}{\overset{r_2}{\rightleftarrows}} 2CO_2 \end{aligned} \tag{11}$$

Westbrook and Dryer (1981) gave the following values for the kinetic parameters:

$$\begin{aligned} r_1 &= 7.59\times10^7\, C_{C_2H_4}^{0.1} C_{O_2}^{1.65} e^{(-15{,}000/T)} \\ r_2 &= 1.26\times10^{10}\, C_{CO}^{1.0} C_{H_2O}^{0.5} C_{O_2}^{0.25} e^{(-20{,}000/T)} \\ r_3 &= 5.0\times10^8\, C_{CO_2}^{1.0} e^{(-20{,}000/T)}. \end{aligned} \tag{12}$$

In the second kinetic rate expression water is a so-called third-body component, which can be seen as a kind of catalyst. Consequently, five continuity equations for mass fractions of species were added to the model, for C_2H_4, O_2, H_2O, CO, and CO_2. The fraction of nitrogen can simply be calculated from an overall mass balance. Because of the source terms with Arrhenius-type kinetics, the equations are stiff and a special numerical procedure was used. The chemistry was decoupled from the flow calculations, and coupling between the two models occurred via the enthalpy, and thus via the temperature. The equations for the mass fraction of the species and the enthalpy equation were solved simultaneously and the results put into the flow equations. Both sets of equations were solved with their own specific time steps in order to keep the numerical procedure stable.

Modeling Results

Explosion diagram

Experiments were performed at different pressures, temperatures, gas flow rates, and tube diameters. The power supply to the wire and the oxygen concentration were varied at constant pressure, temperature, and gas velocity to construct a typical explosion diagram. Calculations were performed in a similar way. This explosion diagram was calculated at pressures of 0.5, 1.0, and 1.5 MPa, temperatures between 298 and 600 K, and gas velocities from 0.5 to 3.0 m/s. A typical example is given in Figure 3, where, in a 21-mm tube at a pressure of 0.5 MPa, a gas temperature of 298 K, and a velocity of 1.5 m/s, the heat flux to the wire and oxygen concentration were varied. The same regions of negligible reaction, local reaction, and explosion were found in the calculations. If a local reaction or explosion occurs, convergence problems have been encountered: a typical calculation takes 15 to 20 h on a single MIPS 10000 processor in a Silicon Graphics Power Challenge computer.

In Figure 3 five different conditions are indicated by points 1 to 5, while the temperature profiles corresponding to these points are given in Figures 11a to 11e. In Figure 11a the heat flux to the wire was 20.7 W and the gas around the wire was heated to temperatures with a maximum of 960 K without ignition of the reaction. The first reaction, given in Eq. 11, has a large activation energy of 123 kJ/mol, so the dependence on temperature is strong. Thus, if the temperature of the wire was too low, this reaction could not be ignited and the gas near the wire was heated by diffusion and convection processes only. Increasing the heat flux to the wire to 22.6 W increased the wire temperature, and now the combustion reactions indeed have been started (see Figure 11b). The calculated temperatures reach values around 2,300 K close to the wire, because of the combined effect of the heat release by the reactions as well as the heat of the wire.

This temperature is higher than the adiabatic temperature rise to 1,775 K for complete consumption of all the oxygen, because the heat supply to the wire continues after ignition.

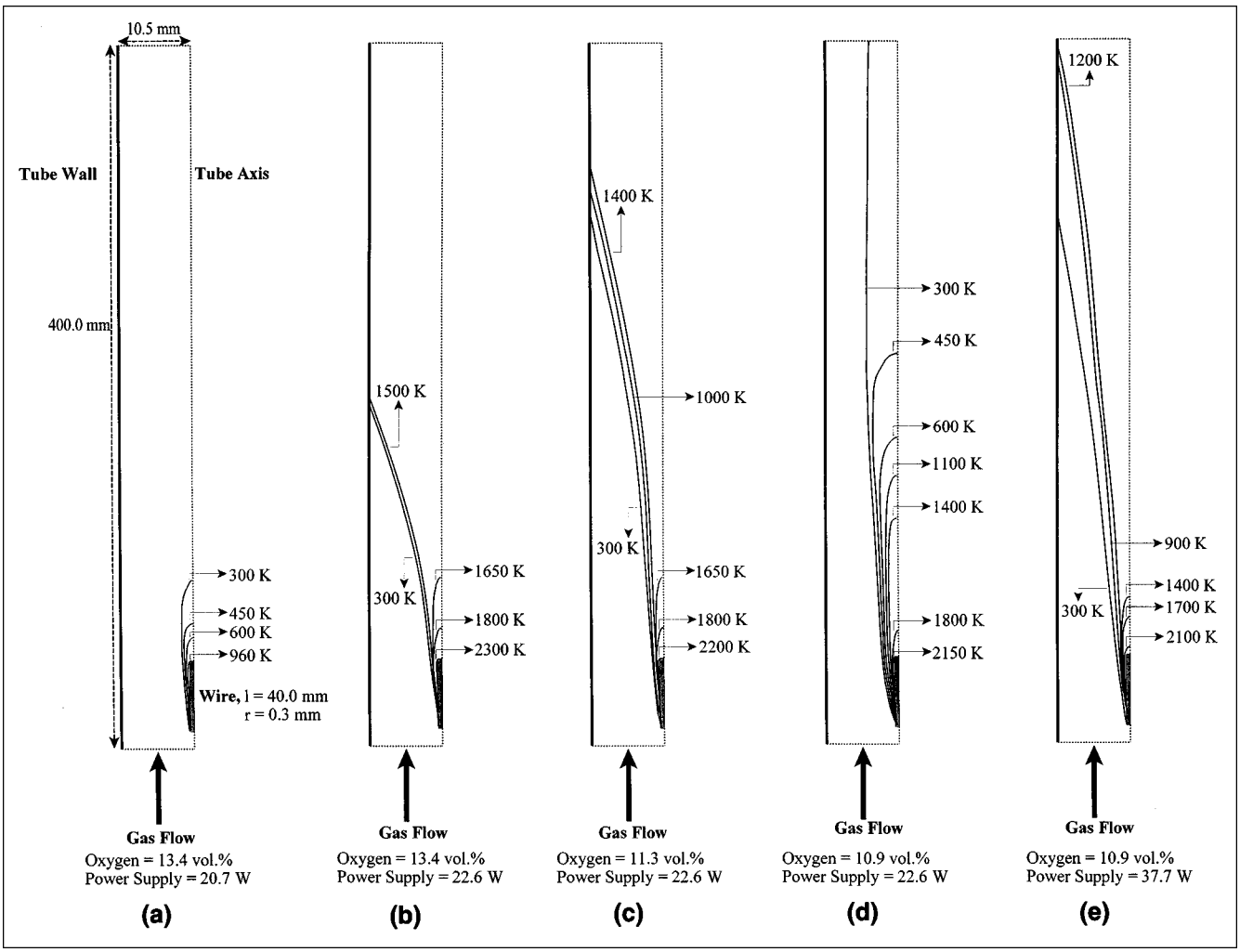

Figure 11. Calculated temperatures as a function of the oxygen concentration and the heat flux to the wire.

Merzhanov and Averson (1971) and Gatica et al. (1987) performed similar calculations for a one-dimensional situation, with either a prescribed temperature or with a constant heat flux as boundary conditions for the hot spot. Temperature distributions similar to ours have been calculated. When ignition is caused by a constant heat flux to the wire, it is not *a priori* known at what temperature the reaction was ignited, because the temperature of the wire surface increases constantly (see also Figures 10 and 13).

After the ignition a reaction front propagates in the upstream direction beyond the wire; all the oxygen is consumed in this front. The reaction zone in the stationary situation is very thin: in Figure 11b over a thickness of about 1.0 mm, the temperature increases to 1,200 K and the oxygen concentration practically drops from 13.4 vol. % to 0.0 vol. %.

At the same heat flux to the wire in point 3, the oxygen concentration has been reduced to 11.3 vol. % (see Figure 11c). This oxygen concentration is now nearer to the explosion point, and downstream of the wire the reaction still goes to completion. The reaction rate is slower compared to the situation given in Figure 11b, because the oxygen concentration in the feed gas is lower; the reaction zone reaches the tube wall at an axial position further downstream and the front is broader. In Figure 11d, the oxygen concentration has been reduced to 10.9 vol. %. In that case a local reaction occurs around the wire, which cannot propagate through the tube anymore, because the heat production by the flame is now completely taken up by the passing cold gas. The reaction was confined to a certain volume, in which the oxygen was completely consumed; we observed a flame of a finite length that never touches the cold wall.

At these conditions a deflagration as in Figure 11b is still possible, provided the heat flux to the wire is increased. This is shown in Figure 11e, where the heat flux is 37.7 W at the same oxygen concentration of 10.9 vol. %. Now an explosion occurs, but the temperature in the reacting zone only reaches 1,200 K and the thickness of the reaction front increases from approximately 1.0 mm to 3.0 mm, due to the decrease in oxygen concentration from 13.4 vol. % to 10.9 vol. %, which decreases the reaction rate and the total amount of energy released.

We also should realize that the required heat fluxes from the wire to the gas are extremely high. For the minimum power input for the situation in Figure 11a the flux is 300

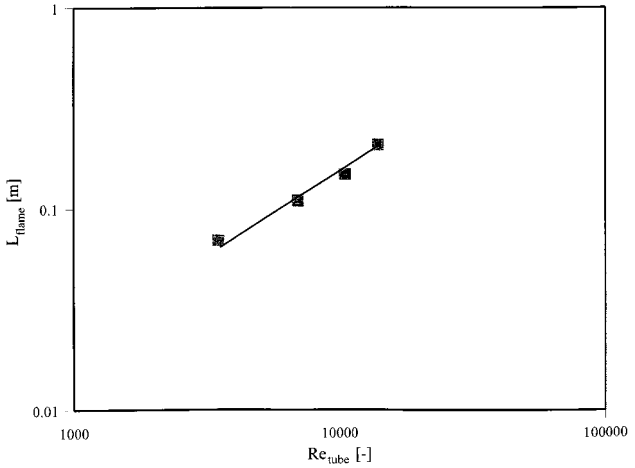

Figure 12. Length of the flame in the local reaction region as a function of the tube Reynolds number.

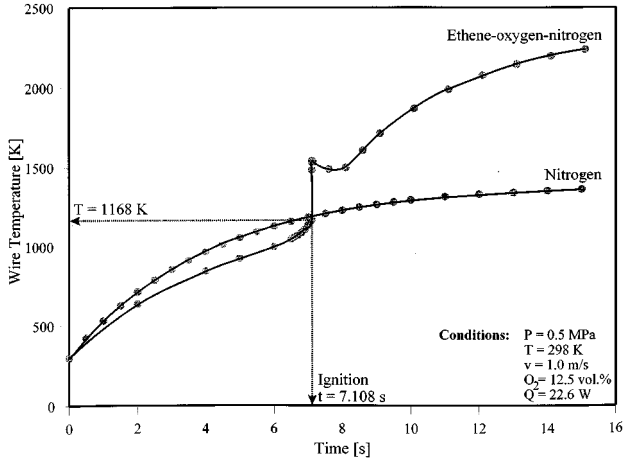

Figure 13. Calculated course in time of the maximum gas temperature in the cells nearest the wire.

kW/m^2, and in Figure 11e it is 500 kW/m^2. Such fluxes are in the order of or higher than the critical maximum heat fluxes in steam boilers, above which the film boiling starts. They are hard to realize locally in closed equipment, unless electrostatic discharges occur.

The size of the local flame given in Figure 11d depends on the oxygen concentration and the gas flow through the tube. Close to the explosion point the flame is relatively long; its size becomes smaller as the oxygen concentration decreases. Furthermore, an increase in gas velocity increases the length of the flame. Calculations were performed in a 21-mm tube at a pressure of 0.5 MPa, gas feed temperatures of 298 K, and oxygen concentrations that are 0.1 vol. % below the explosion point. In Figure 12 the calculated length of the flame is plotted as a function of the Reynolds number through the tube. All oxygen was consumed in the flame. In our calculations, therefore, we have taken, perhaps rather arbitrarily, the length of the oxygen-free zone as the length of the flame. An increase in gas velocity increases the length, and we found $L_{\text{flame}} \approx Re^{1.0}$.

Propagation in time of an explosion

The development in time of an explosion is given in Figures 13 and 14. A mixture containing 12.5 vol. % oxygen was ignited in a 21-mm tube with a heat flux to the wire of 22.6 W, conditions that are well within the explosion range, at a pressure of 0.5 MPa, a feed gas temperature of 298 K, and a gas velocity of 1.0 m/s. Figure 13 shows the course of the maximum gas temperature in the cells nearest in time to the wire. At the start the wire was heated with a constant heat flux. After $t = 6.0$ s, the cells near the wire reached a temperature of 900–1,000 K, and the combustion reaction began, resulting in additional heat and a more rapid increase in temperature. After $t = 7.1$ s and at a temperature of 1,168 K the reaction rate became so fast that a sudden jump in the temperature to 1,540 K occurred, while simultaneously a reaction front started to propagate through the tube. This ignition occurred within a time period of 1 ms. After $t = 8.0$ s, the temperature increased further, because the heat flux to the wire was not stopped after the ignition. Also, in Figure 13 the temperature is given for the same heat flux and for nitrogen flow through the tube. The cells near the wire reach a constant temperature of 1,370 K, at which point the heat production and removal are balanced. We observe that the temperature increases more rapidly in a nitrogen mixture: its heat capacity is approximately 10% lower than for the gas mixture containing ethene.

In Figures 14a to 14f, the propagation of this front is given as a function of time as from the ignition at $t = 7.108$ s and up to 20 ms, 37 ms, 52 ms, 57 ms, and 100 ms later, respectively. The reaction started in the wake of the wire; as time passed the reaction expanded in the radial and axial direction and the propagation rate increased. All the oxygen was consumed in the reaction zone, and a final temperature of 1,500 K was reached. This is the same temperature that Zabetakis (1965) found experimentally, as we did in our experiments (see Bolk and Westerterp, 1998). Finally, the stationary situation looks very similar to Figure 11b.

Discussion

Comparison between experiments and calculations

The explosion diagram of Figure 3 has been calculated at different pressures, gas feed temperatures, and velocities in the 50-mm tube, and the minimum heat flux to the wire and the critical oxygen concentration in the explosion point were determined.

Minimum Heat Flux and Ignition Temperature. In Figure 15 the minimum heat flux to the wire, as determined by calculations or in experiments in the 50-mm tube, expressed in MW/m^2 wire surface, are plotted as a function of the tube Reynolds number. An increase in the tube Reynolds number increases the required minimum heat flux to the wire, because of the better heat transfer from the wire. Consequently, a higher heat flux is necessary to reach a certain minimum ignition temperature. The calculated and experimentally measured minimum heat fluxes show the same dependence on the Reynolds number, although the absolute

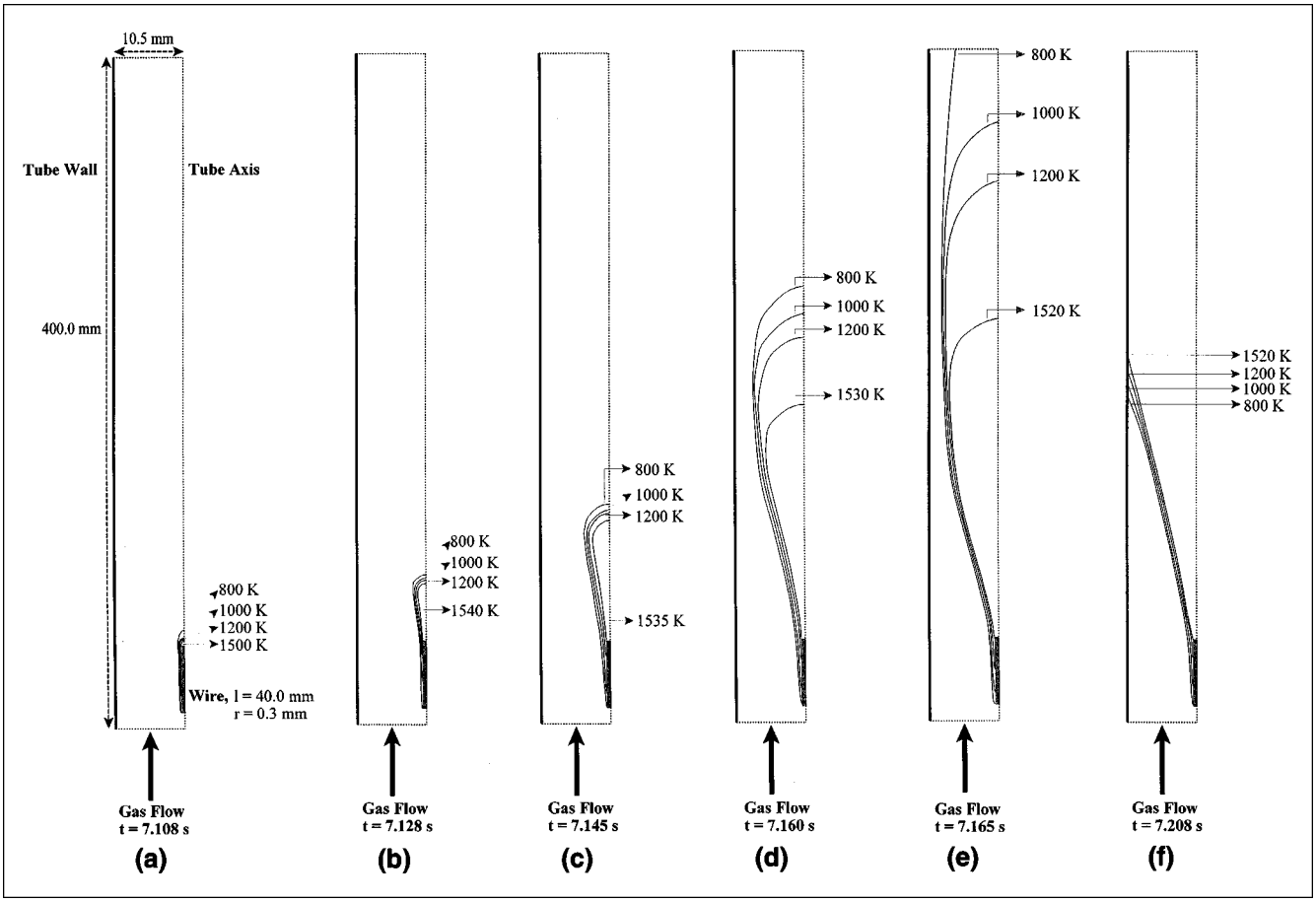

Figure 14. Propagation of the reaction through the tube at ignition and onward at 20, 37, 52, 57 and 100 ms later, respectively.

values differ. Furthermore, an increase in pressure leads to a decrease in the experimental and calculated minimum heat fluxes. At pressures of 0.5 and 1.0 MPa the measured heat fluxes are higher than the calculated ones. Experimentally, the total amount of heat transferred from the wire to the gas is lower than the value given in Figure 15, because part of the heat produced in the wire is lost to the connecting rods as well as in radiation to the tube wall. These effects have not been incorporated into the model. At a pressure of 1.5 MPa the calculated minimum heat flux is higher than the experimental one. A sharp decrease of the required minimum heat flux to the wire has been observed experimentally, at this pressure, and probably is caused by a change in the chemical reactions and/or their kinetics at these pressures.

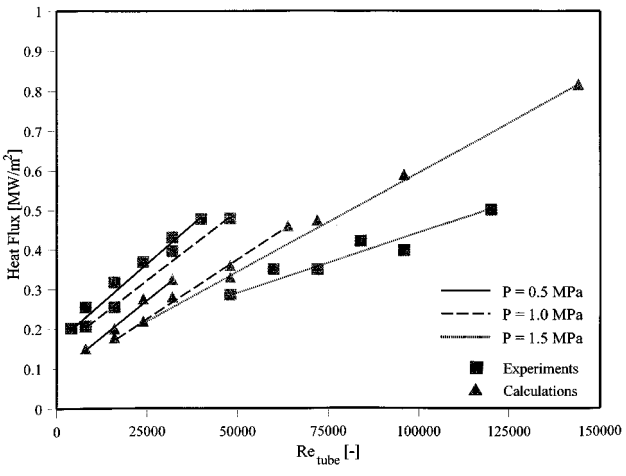

Figure 15. Calculated vs. experimental minimum heat flux in the 50-mm tube as a function of the tube Reynolds number.

For safety reasons, it is very important to know the temperature of the wire at ignition. Platinum and nickel wires with a length of 40.0 mm and a diameter of 0.5 mm have been placed vertically in the tube and their temperature has been measured during an experiment. Experimentally measured courses in time of the wire temperature look very similar to Figure 10. Initiation of heterogeneous reactions on the wire surface has been observed at relatively low temperatures. In Table 3, the wire temperature is given for some conditions at which these heterogeneous reactions were initiated. This initial temperature is not influenced by the gas velocity, so the reactions must have started on the surface and must therefore be independent of the hydrodynamics. A

Table 3. Temperature of the Wire at Which Heterogeneous Reactions Start*

Wire Material	Exp. Conditions	Ignition Temp. [K]
Nickel	$P = 0.5$ MPa $\upsilon = 0.25, \ldots, 1.0$ m/s	675, …, 685
	$P = 1.0$ MPa $\upsilon = 0.25, \ldots, 1.0$ m/s	665, …, 675
Platinum	$P = 0.5$ MPa $\upsilon = 0.25, \ldots, 1.0$ m/s	675, …, 725
	$P = 1.0$ MPa $\upsilon = 0.25, \ldots, 1.0$ m/s	675, …, 725

*$T_{gas} = 298$ K.

pressure increase from 0.5 MPa to 1.0 MPa decreases the first temperature by about 10 K. Once these heterogeneous reactions have been started, additional heating of the wire occurs. Further, for wire temperatures above 1,000 K homogeneous reactions also start to occur. The temperature of the wire at ignition also has been calculated by the model. In Figure 16a this temperature is given as a function of the gas velocity through a 21-mm tube at pressures of 0.5, 1.0 and 1.5 MPa, respectively. The calculated temperatures are considerably higher than the measured temperatures given in Table 3. The temperatures are calculated by the model as those required to initiate the first homogeneous reaction of the adopted two-step reaction mechanism. The heterogeneous reactions have not been taken up in the model, and therefore we cannot expect the results of the calculations and experiments to coincide.

The overall heat-transfer coefficient from the wire to the gas can be represented by a general Nusselt-type of relation:

$$Nu = \frac{\alpha d_w}{\lambda_g} = \text{constant } Re_w^{(0.6-0.8)} Pr^{1/3}. \qquad (13)$$

For gases, the Prandtl number is approximately 1. The heat transfer from the wire to the gas can be represented as

$$Q_{w \to g} = \alpha A (T_w - T_g). \qquad (14)$$

In Figure 15 we see that the Q/A increases linearly with the flow rate through the tube, and therefore we can write the temperature of the wire as

$$T_w = T_g + \frac{Q_{w \to g}}{\alpha A} = T_g + \frac{Q_0 + B Re_w}{(\lambda_g / d_w) Re_w^{0.7} Pr^{1/3}}. \qquad (15)$$

An increase in gas velocity leads to a higher Reynolds number and, according to Eq. 15, the temperature of the wire must be higher to bring the gas temperature close to the wire to a level where an explosion is initiated (see Figure 16a).

In Figure 16b, the same calculated wire temperatures are now given as a function of the Reynolds number based on the length of the wire. Equal Reynolds numbers lead to equal heat-transfer coefficients. At increasing pressures, however,

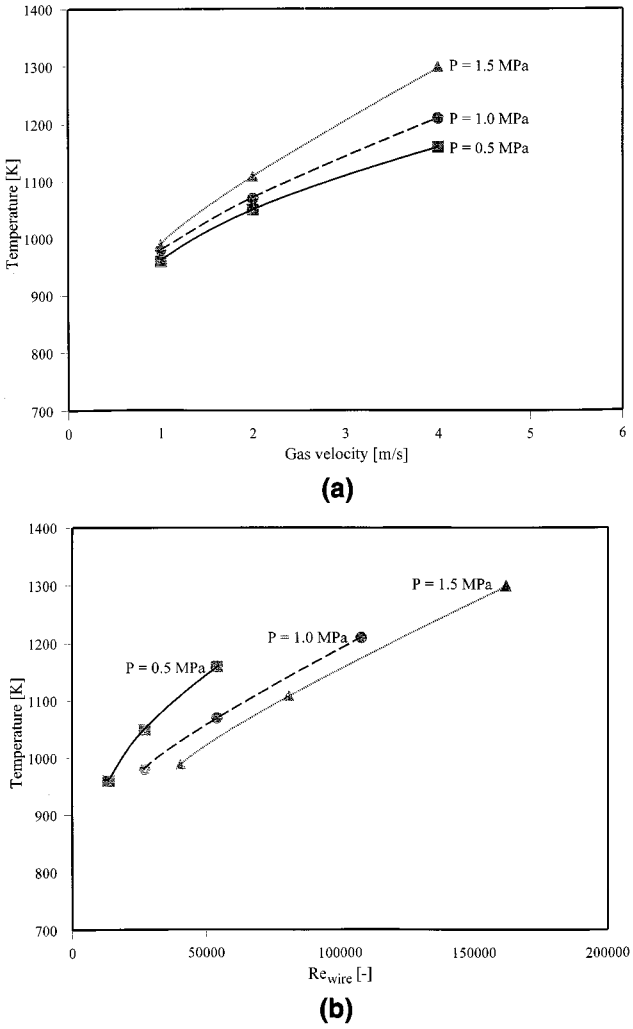

Figure 16. Wire temperature at ignition as calculated by the model as a function of the gas velocity and Reynolds number based on the length of the wire.

the reaction rate will be increased. This will lead to a decrease in the gas temperature required for an explosion, and thus of the wire temperature at initiation (see Figure 16b).

The wire temperature at ignition can be estimated with the help of a Damköhler number (Da) which gives the ratio between the chemical reaction time for the first reaction of our two-step scheme and the contact time of the gas flowing along the wire, defined by

$$Da = \frac{\tau_{\text{contact}}}{\tau_{\text{chemical}}} = \frac{r_{1,0} L}{u C_{O_2,0}}$$

$$= \frac{7.59 \times 10^7 \, e^{(-15{,}000/T)} C_{C_2H_4,0}^{0.1} C_{O_2,0}^{1.65} L}{u C_{O_2,0}} = \frac{k C_{C_2H_4,0}^{0.1} C_{O_2,0}^{0.65} L}{u}. \qquad (16)$$

For the oxygen to be reacted away 99% under isothermal

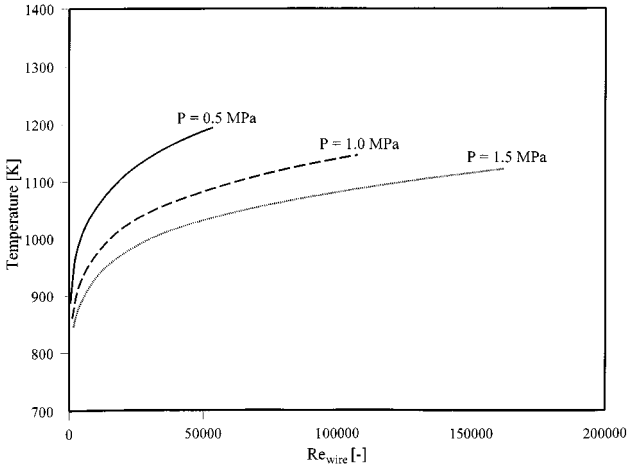

Figure 17. Wire temperature at ignition as calculated by Eq. 17 for $Da = 30$.

Gas composition: $O_2 = 12.5$ vol. % and $C_2H_4 = 25$ vol. %.

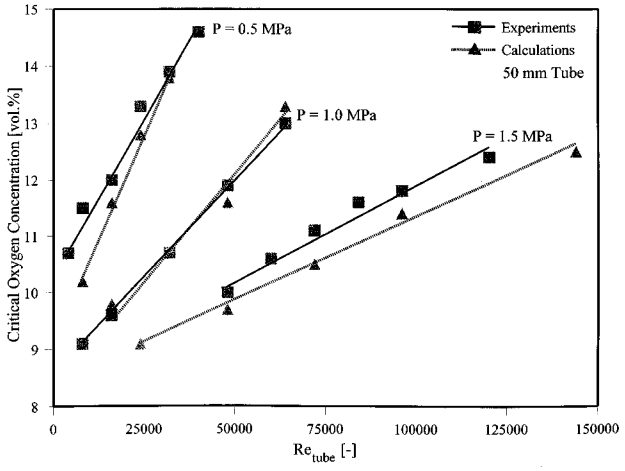

Figure 18. Critical oxygen concentration in the explosion point in the 50-mm tube.

conditions, the value of Da must be 30 or higher. This leads to

$$T_{\text{init}} = \frac{-15{,}000}{\ln\left(\dfrac{uDa}{k_\infty C_{C_2H_4,0}^{0.1} C_{O_2,0}^{0.65} L}\right)} = \frac{+15{,}000}{\ln\left(\dfrac{k_\infty C_{C_2H_4,0}^{0.1} C_{O_2,0}^{0.65} L d_w \rho}{30\, Re_w \mu}\right)}. \quad (17)$$

In Figure 17, the initiation temperature as calculated by Eq. 17 for $Da = 30$ is given as a function of the Reynolds number based on the length of the wire. An increase in Reynolds number demands a higher wire temperature and an increase in pressure for a lower temperature. The temperatures calculated with Eq. 17 are in the same range as the temperatures calculated by the model and given in Figure 16b.

Critical Oxygen Concentration in the Explosion Point. In Figure 18 the experimental and calculated critical oxygen concentrations at the explosion point for pressures of 0.5, 1.0, and 1.5 MPa are compared for different tube Reynolds numbers. The agreement between the model and the calculations is good, especially since we have used data from the literature, and have not fitted the kinetic parameters of the model to the experimental data. We have used the values proposed by Westbrook and Dryer (1981), who used completely different experimental conditions. The reason why the kinetics in our case fit so well is not exactly known. We observe the same linear relation of the critical oxygen concentration in the upper explosion limit to the tube Reynolds number, and also that an increase in pressure decreases the critical oxygen concentration in the explosion point. Thus, the explosion region widens. Calculations at gas velocities above 3.0 m/s are difficult to make, because of the very long computation times caused by the convergence problems.

Finally, the effect of the temperature was investigated. Calculations were performed in the 50-mm tube at a pressure of 1.5 MPa for gas feed temperatures up to 600 K at Reynolds numbers of 48.000 and 96.000, respectively: results are given in Figure 19. Again the agreement between the model and the experiments is good, and the linear decrease in the critical oxygen concentration with temperature is confirmed by the calculations. Our calculations resulted in a flame temperature of around 1,500 K, which is equal to the experimentally determined value.

Effect of flow rate

The critical oxygen concentration at the upper explosion limit increases linearly with the flow rate through the tube. If the critical oxygen concentration in mole per unit volume is plotted as a function of the Reynolds number, the line has the same slope at different pressures (see Figure 20). Heat removal occurs in a stagnant medium by molecular diffusion,

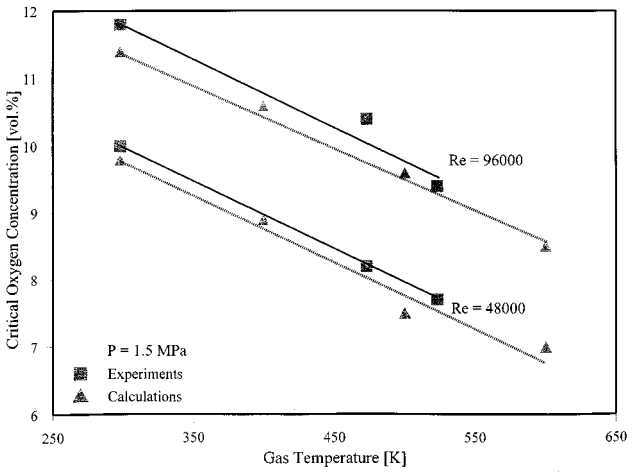

Figure 19. Effect of temperature on the critical oxygen concentration in the explosion point.

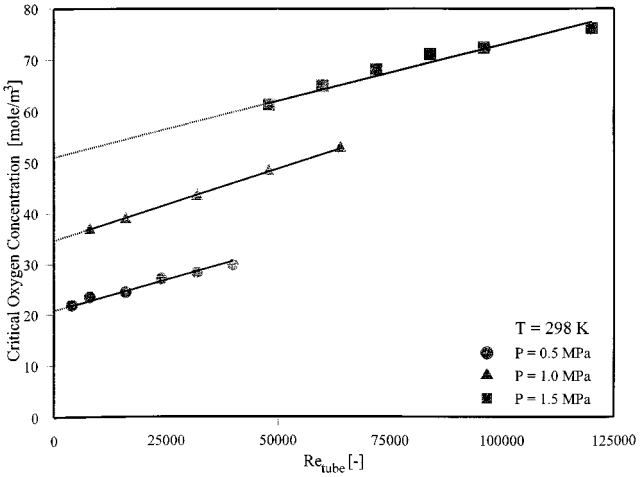

Figure 20. Influence of pressure on critical oxygen concentrations in the explosion point.

Oxygen concentration in moles per unit volume.

conduction, and free convection. In a flowing medium at high Reynolds numbers added to these is the heat removal due to turbulent transport. In highly turbulent flows this transport mechanism normally dominates the other ones. To obtain ignition this additional heat removal must be compensated for, so the heat production rate must be increased, which causes the critical oxygen concentrations at the explosion point to increase.

Our computational fluid dynamics (CFD) calculations show that in the region close to the explosion point a flame has developed around the hot wire. This is because this stationary flame shows that the heat production rate (HPR) equals the heat withdrawal rate (HWR); thus HPR = HWR. So, at any Reynolds number, $\mathrm{HPR}_{Re} = \mathrm{HWR}_{Re}$, and on the boundary line we have that HPR suddenly becomes larger than HWR. Further, in a stationary flame in a gas with an excess of ethene we can assume that the key compound, oxygen, is completely consumed, so $\mathrm{HPR} = \phi_v \Delta H_{\mathrm{comb}} C_{\mathrm{O}_2}$. The gas flowing around the flame removes all this heat, so $\mathrm{HWR} = \alpha A(T_{\mathrm{flame}} - T)$.

In classic theories an overall heat-transfer coefficient relates to distinct boundaries over which heat transfer takes place. This is not the case for a local flame in a flowing gas, which occupies only a fraction of the tube cross section. In principle the α can be estimated as the heat conductivity of the medium divided by the characteristic length of the transfer area. In our case, we assume that the heat transport takes place from the flame to the gas flowing around this flame, and that the characteristic length can be approximated by the thickness of the reaction zone in the flame front, δ_{flame}.

In a flowing gas, the heat withdrawal rate will increase with higher gas flow rates, and to reach critical conditions for flame propagation, the heat production rate must also increase, and therefore the oxygen concentration increases. We assume that the critical condition in a flowing gas can be given as

$$\left(\phi_v \Delta H_{\mathrm{comb}} C_{\mathrm{O}_2}\right)_{Re} = \alpha_{\mathrm{eff}} A(T_{\mathrm{flame}} - T), \qquad (18)$$

in which ϕ_v is the volumetric rate of the gas feed to the flame.

If we now assume that the effective heat-transfer coefficient in a flowing medium consists of the heat-transfer coefficient in a stagnant medium plus a contribution due to the gas flow rate, we can write:

$$\alpha_{\mathrm{eff}} = \frac{\lambda_{\mathrm{eff}}}{\delta_{\mathrm{flame}}} = \frac{\lambda_{\mathrm{turb}}}{\delta_{\mathrm{flame}}} + \frac{\lambda_g}{\delta_{\mathrm{flame}}} \approx \frac{\lambda_{\mathrm{turb}}}{\delta_{\mathrm{flame}}} + \alpha_{Re\to 0}. \qquad (19)$$

The second term on the righthand side of Eq. 19 is representative for the HWR in a stagnant gas. Its value can be estimated on the basis of the $\mathrm{HPR}_{Re\to 0}$, because $\mathrm{HPR}_{Re\to 0} = \mathrm{HWR}_{Re\to 0}$. The $\mathrm{HPR}_{Re\to 0}$ approaches the heat production rate in a mixture of gas with the oxygen content as determined for explosions in an autoclave with stagnant gas. This finally leads to

$$\phi_v \Delta H_{\mathrm{comb}}\left(C_{\mathrm{O}_2,Re} - C_{\mathrm{O}_2,Re\to 0}\right) \approx \frac{\lambda_{\mathrm{turb}}}{\delta_{\mathrm{flame}}} A(T_{\mathrm{flame}} - T). \qquad (20)$$

This relation holds up to the explosion limit. Of course, $\lambda_{\mathrm{turb}}/\delta_{\mathrm{flame}} \cdot A$, being an overall value, has to be further determined. As already explained, the flame temperature, T_{flame}, has a constant value within a certain accuracy margin. From our experiments we have to determine what the relevant parameters determining $\lambda_{\mathrm{turb}}/\delta_{\mathrm{flame}} \cdot A$ are. We first switch to mole fractions, using the relation $C_{\mathrm{O}_2} = X_{\mathrm{O}_2} P/RT$, in which P is the system pressure and $T = T_{\mathrm{flame}}$, because the relevant concentration is that in the flame. This leads us to

$$\left(X_{\mathrm{O}_2,Re} - X_{\mathrm{O}_2,Re\to 0}\right) \approx \frac{RT_{\mathrm{flame}} \dfrac{\lambda_{\mathrm{turb}}}{\delta_{\mathrm{flame}}} A(T_{\mathrm{flame}} - T)}{PuS\Delta H_{\mathrm{comb}}}. \qquad (21)$$

The turbulent heat conductivity was introduced in Eq. 19. In general, turbulence transports heat and mass as rapidly as momentum (see Hinze, 1975). As in the molecular gas theory, the turbulent viscosity, turbulent conductivity, and turbulent diffusivity are coupled to a typical turbulence length scale and to a turbulent velocity (Schlichting, 1968; Tenneckes and Lumley, 1972; Nieuwstadt, 1992):

$$\lambda_{\mathrm{turb}} \sim \rho C_p \delta_{\mathrm{turb}} u'. \qquad (22)$$

Turbulent velocity fluctuations in a pipe normally scale with the mean velocity, and the characteristic turbulence length scale will depend on the tube diameter (see Bird et al., 1960; Raymond and Amundson, 1964; and Nieuwstadt, 1992). Therefore, the turbulent heat conductivity can be approximated by

$$\lambda_{\mathrm{turb}} \sim \rho C_p d_{\mathrm{tube}} \bar{u}. \qquad (23)$$

We can introduce the external surface of a cylinder for A, if we approach the shape of the flame by its equivalent cylinder shape. So, $A = \pi d_{\mathrm{flame}} L_{\mathrm{flame}}$ and S is the cross-sectional area of this flame, equal to $\pi/4 \cdot (d_{\mathrm{flame}})^2$. The shape and size will be determined by the existing combustion reactions. The length of the flame will depend on the kinetics and the veloc-

ity through the tube, but in general,

$$\frac{A}{S} \approx \left(\frac{4L}{d}\right)_{\text{flame}}. \tag{24}$$

This eventually leads to the following relation for the increase in the mole fraction oxygen required for flame propagation in a flowing gas:

$$\left(X_{O_2,Re} - X_{O_2,Re\to 0}\right) \sim \frac{RT_{\text{flame}}C_p}{P\Delta H_{\text{comb}}}\left(T_{\text{flame}} - T\right)\frac{\rho d_{\text{tube}}}{\delta_{\text{flame}}}\left(\frac{L}{d}\right)_{\text{flame}}, \tag{25}$$

where δ_{flame} will probably depend on the kinetics. For our system the shape of the flame has been determined by CFD calculations (see Figures 11 and 12). In general, we can state that the flame diameter is only a few millimeters and independent of the tube diameter, and that the length will depend on the velocity through the tube. It was found by calculations that $X_{O_2,Re} - X_{O_2,Re\to 0} \approx Re^{1.0}$. This means that $(\rho d_{\text{tube}}/\delta_{\text{flame}})\cdot(L/d)_{\text{flame}} \approx Re^{1.0}$. Thus we eventually obtain

$$\left(X_{O_2,Re} - X_{O_2,Re\to 0}\right) = \beta\frac{RT_{\text{flame}}C_p}{P\Delta H_{\text{comb}}}\left(T_{\text{flame}} - T\right)Re^{1.0}. \tag{26}$$

We realize that this derivation is based on many assumptions and that the viscosity has not been varied in our experiments. We use our experimental data to evaluate this relation. The critical oxygen concentrations at a zero flow rate for the experiments at increased temperatures have been found by extrapolation to be similar to those in Figures 6 and 20. In Table 4, the values obtained in this manner are compared with data in the literature on explosion limits in stagnant ethene–air–nitrogen mixtures at increased temperatures. The correspondence is not as good as for the experiments at room temperature (see Table 2). We also use the data obtained in the two other test tubes with diameters of 21 and 100 mm, respectively. Some results have been presented by Bolk et al. (1996), and others will be presented in a later study. The best fit for β equals 1.53×10^{-3} kg/m^3, and this finally leads to Eq. 27:

$$\left(X_{O_2,Re} - X_{O_2,Re\to 0}\right) = 1.53\times10^{-3}\frac{RT_{\text{flame}}C_p}{P\Delta H_{\text{comb}}}\left(T_{\text{flame}} - T\right)Re^{1.0}. \tag{27}$$

Figure 21 contains a parity plot of the experimental and calculated $(X_{O_2,Re} - X_{O_2,Re\to 0})$ up to Reynolds numbers of 125,000. For Reynolds numbers between 10,000 and 125,000 the data can be correlated with a standard deviation of 12% in the value of $(X_{O_2,Re} - X_{O_2,Re\to 0})$. At lower Reynolds numbers and for the 100-mm tube the correlation is less accurate, because here free convection intervened with an accurate determination of the critical oxygen concentration. Further, we should realize that Eq. 27 only holds for deflagrations and *not* for detonations.

Table 4. Critical Oxygen Concentrations at $Re \to 0$ vs. Experimental Results in Quiescent Mixtures*

P [MPa]	T [K]	Crit. Oxygen Conc. [Vol. %]	Reference
0.5	373	10.1	Hashiguchi et al. (1966)
	423	9.5	This work
		10.0	Craven and Foster (1966)
		8.8	Fiumara and Cardillo (1976)
	473	8.8	Gaube et al. (1968)
	498	9.0	This work
	523	6.4	Craven and Foster (1966)
	573	8.4	This work
1.0	373	8.8	Hashiguchi et al. (1966)
	423	8.0	This work
		7.0	Fiumara and Cardillo (1976)
		7.0	Craven and Foster (1966)
	473	7.8	Gaube et al. (1968)
	498	6.9	This work
	523	5.4	Craven and Foster (1966)
1.5	423	5.6	Craven and Foster (1966)
		5.7	Fiumara and Cardillo (1976)
	473	6.6	This work
		7.3	Gaube et al. (1968)
	523	6.2	This work
2.0	373	6.3	Hashiguchi et al. (1966)
	523	6.0	Crescitelli et al. (1979)

*Increased temperatures.

Potential ignition sources in plant operation

Different ignition sources can be present in ethene oxidation plants, which can lead to dangerous situations. During plant operation, the silver-based catalyst will age and catalyst dust may be carried out of the reactor and precipitate at places of low gas velocities. Heterogeneous reactions may be initiated at the surface of these dust particles at temperatures as low as 650–700 K, because silver will show about the same catalytic activity as platinum or nickel (see Table 3). Once such a reaction has started, the local temperature will increase gradually, and at temperatures exceeding 850 K homogeneous reactions also may be initiated (see Figure 17). In

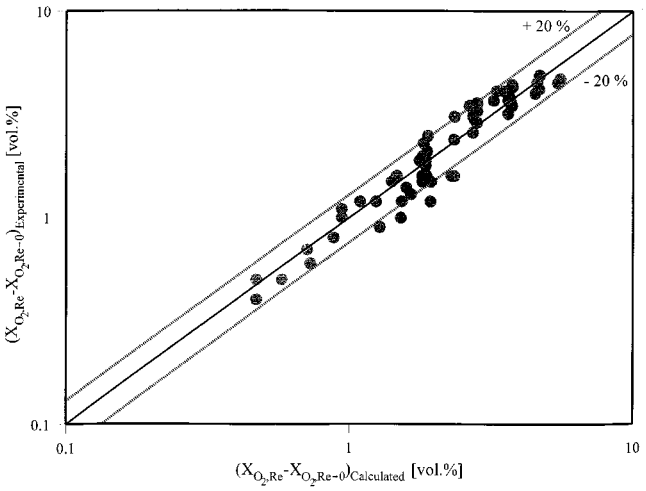

Figure 21. Parity of the experimental and calculated $[X_{O_2,Re} - X_{O_2,Re\to 0}]$.

dead zones with no gas flowthrough, such reactions die out because of oxygen starvation (see Bolk et al., 1999). In zones with a low gas flowthrough, these reactions may propagate and finally lead to an explosion wave traveling through all the connected equipment.

At the reactor outlet glycol and polyglycols also may be present, due to the reaction between ethene oxide and water, formed by further oxidation of ethene, and also by polymerization between ethene oxide and (poly)glycols. These are exothermic reactions, which may create local hot spots. Where there is low gas velocity, hot-spot temperatures of over 850 K can initiate homogeneous reactions, which can develop into an explosion. Once the reactions are initiated, the temperatures near the hot spot may rise to above 2,000 K. This will eventually lead to carbon formation and to decomposition of the glycol. Heterogeneous reactions, for example, on catalyst dust deposits in downstream equipment, may even evoke an ignition at temperatures around 700 K. Luckily, very large heat fluxes are necessary in a flowing gas to reach such temperatures (see Figure 15). These heat fluxes are at least an order of magnitude larger than those normally present in closed equipment, such as in heat exchangers. In normal plant operation such conditions will hardly occur.

In ethene oxidation plants the occurrence of decompositions is a well-known problem. We think these decompositions are initiated by local hot spots that are created by local reactions in zones of low gas flowthrough, which may ignite a local combustion reaction. Combustion reactions then propagate, but they will die out in the downstream equipment or pipelines, where gas velocities are high again.

Conclusions

Explosion limits for reactive gaseous mixtures cannot be given, because they are influenced by many parameters related to the initial conditions (pressure and temperature), to the physical environment (shape and size of the vessel or tube), and to the characteristics of the ignition source. Above all we have shown that the explosion limits also depend on the hydrodynamics of the system.

In flowing systems the explosion region becomes smaller the faster the gas flows, due to the additional heat and mass transfer from the reaction front. Increasing the flow rate results in an increase in the critical oxygen concentration. This means that the explosion region becomes narrower. Experiments in quiescent gas mixtures give the lowest critical oxygen concentration at the upper explosion limit, making it the worst-case situation. In stagnant gas at ambient temperature and atmospheric pressure the explosion limits have been determined, and the influence of vessel geometry and ignition source are well documented. However, these results cannot be used to design industrial processes, which is to say, they lead to a too conservative approach.

We could distinguish clearly between ignition and the propagation of the reaction through the tube. The minimum power supply rate to the wire for an ignition was determined, as were increases for all wires and wire orientations at increasing gas flow rates. Once the gas mixture is ignited, two different effects can occur. If the oxygen concentration in the gas mixture is too low, the reaction is localized around the heated wire and we have a local, stabilized flame. Propagation of the reaction is not possible, because the reaction heat produced is balanced by the heat loss. Increasing the oxygen concentration causes an increase in the heat production rate and elongation of the flame; eventually and at a certain concentration the local reaction around the wire is no longer balanced by the heat loss, so the reaction can propagate through the tube. This point is defined as the explosion point, provided the power supply is at its minimum.

Oxygen concentration at the explosion point is almost constant for different wires, it only depends on the experimental conditions such as temperature, pressure, and flow rate. Increasing the pressure and/or the gas temperature causes a decrease in the critical oxygen concentration. This means that the explosion region becomes larger. Varying the excess of ethene has only a slight effect on the explosion limits. This can be explained by taking the total heat capacity of the gas mixture into account. Extrapolation to zero velocity gives critical oxygen concentrations that are comparable with the concentrations found in experiments with stagnant mixtures.

The experimentally obtained results have been modeled using a commercial computational fluid dynamics program. In a cylinder-symmetrical, two-dimensional model the gas was ignited by a vertically placed hot wire. In the model only homogeneous reactions were taken into account. The reaction scheme used consists of two consecutive reactions, and their kinetic parameters were taken as originally proposed by Westbrook and Dryer (1981). The first reaction gives the oxidation of ethene to water and carbon monoxide, and the second reaction delineates the equilibrium reaction of the oxidation of carbon monoxide to carbon dioxide. This scheme predicts the heat production rate better than a one-step, total combustion scheme, which overestimates the heat released. The k-ϵ turbulence model was used to describe the turbulence, while the interaction between the turbulent flow and the chemistry was neglected.

The developed model describes the experimentally observed phenomena well. At a prescribed pressure, gas feed temperature, and gas velocity the regions of negligible reaction, local reaction, and explosion can be distinguished in a plot of the heat flux to the wire and the oxygen concentration in the gas mixture. The minimum heat flux needed to ignite the reaction is a function of the gas velocity and the pressure and is independent of the oxygen concentration. The calculated value of the heat flux deviates from the experimentally measured value, because the experimentally observed heterogeneous reactions were neglected in the model. The same linear dependence on the tube Reynolds number was found, as was the same dependence on pressure. The critical oxygen concentration required for flame propagation depends on the velocity, pressure, temperature, and tube size just as it is when determined experimentally. The developed model can be used to calculate the critical conditions in other situations, making additional experimental superfluous. Above all, we think the model also can be used to calculate critical conditions for other gas mixtures, if the overall combustion kinetics are known.

The results obtained in this study can be used to redesign partial oxidation plants, such as the partial oxidation of ethene to ethene oxide, because they apparently can be safely operated with higher oxygen concentrations, provided the gas is kept flowing and the flow rates are high.

Acknowledgments

These investigations were supported by the Netherlands' Foundation for Chemical Research (SON) with financial aid from the Netherlands' Technology Foundation (STW). The work forms part of a project initiated by the University of Twente, Dow Benelux N.V. at Terneuzen, and Shell International Chemicals B.V. at The Hague, The Netherlands. The authors wish to thank M. Cos, R. van Zinderen Bakker, G. M. Stapelbroek, and A. M. Boerlage for performing part of the experimental work, and F. ter Borg, G. H. Banis, P. J. Flanagan and A. H. Pleiter for technical support. They also want to thank M. Kremers and G. M. Bos for performing preliminary calculations, and J. A. M. Kuipers and J. B. W. Kok for fruitful discussions. Finally, J. M Wigman, R. Schurink, and H. van den Berg of Dow, and J. P. van der Linden, M. van der Schoot, and G. H. Geertsema of Shell are gratefully acknowledged for their guidance and support.

Notation

A = area (m^2)
B = constant in Eq. 15 (W/m^2)
c, C = concentration (mol/m^3)
C_p = heat capacity ($J/kg \cdot K$)
d = diameter (m)
D = diffusion coefficient (m^2/s)
g = 9.81, gravity constant (m^2/s)
H = total enthalpy, consists of internal (h) and kinetic energy (J/kg)
J = mass flux ($kg/s \cdot m^2$)
k = homogeneous reaction velocity constant ($m^{3(n-1)}/mol^{(n-1)}s$)
k_∞ = preexponential factor ($m^{3(n-1)}/mol^{(n-1)}s$)
M = molecular mass (kg/mol)
p = pressure (N/m^2)
q = energy flux (W/m^2)
Q = heat release rate (W/m^3)
R = gas constant, 8.314 ($J/mol \cdot K$)
r_i = reaction rate of reaction i ($mol/m^3 \cdot s$)
t = time (s)
u = velocity (m/s)
Y = species mass fraction
β = constant in Eq. 26 (kg/m^3)
δ_{ij} = Kronecker delta (1 for $i = j$, otherwise 0)
κ = bulk viscosity in Eq. 5 ($Pa \cdot s$)
λ = thermal conductivity ($W/m \cdot K$)
μ = viscosity ($Pa \cdot s$)
τ = viscous stress tensor ($kg/s^2 \cdot m$); residence time (s)

Subscripts and superscripts

chemical = chemical induction time
contact = contact time between the gas and the wire
init = initiation
L = laminar
ns = total number of species
0 = initial conditions, zero flow rate
room = ambient temperature
R = reaction
s = of species s
sol = solid
tube = tube
1, 2, 3 = reaction number
$\bar{}$ = average
$'$ = fluctuations

Literature Cited

Beek, W. J., and K. M. K. Muttzall, *Transport Phenomena*, Wiley, Chichester (1975).
Bird, R. B., W. E. Stewart, and E. N. Lightfoot, *Transport Phenomena*, Wiley, New York (1960).
Birkan, M. A., and C. K. Law, "Asymptotic Simulation of the Four-Step Global Kinetics of Hydrocarbon-Air Mixtures Under Flow Reactor Conditions," *Combust. Sci. Tech.*, **51**, 145 (1987).
Bolk, J. W., N. B. Siccama, and K. R. Westerterp, "Flammability Limits in Flowing Ethene-Air-Nitrogen Mixtures: An Experimental Study," *Chem. Eng. Sci.*, **10**, 2231 (1996).
Bolk, J. W., F. ter Borg, and K. R. Westerterp, "Explosion Limits in Flowing Ethene-Air-Nitrogen Mixtures: Effect of Tube Size and Obstacles," in press (1999).
Borghi, R., "Turbulent Combustion Modelling," *Prog. Energy Combust. Sci.*, **14**, 245 (1988).
Burgess, M. J., and R. V. Wheeler, "The Lower Limit of Inflammation of Mixtures of the Paraffin Hydrocarbons with Air," *J. Chem. Soc.*, **99**, 2013 (1911).
Chen, L. D., and G. M. Faith, "Ignition of a Combustible Gas Near Heated Vertical Surfaces," *Combust. Flame*, **42**, 77 (1981).
Chippett, S., "Flammability Measurements in a Turbulent Flow System," AIChE Loss Prevention Symp., Session on Materials Reactivity and Flammability (1993).
Cho, P., and C. K. Law, "Catalytic Ignition of Fuel/Oxygen/Nitrogen Mixtures over Platinum," *Combust. Flame*, **66**, 159 (1986).
Coward, H. F., and P. G. Guest, "Ignition of Natural Gas-Air Mixtures by Heated Metal Bars," *J. Amer. Chem. Soc.*, **49**, 2479 (1927).
Craven, A. D., and M. G. Foster, "The Limits of Flammability of Ethylene in Oxygen, Air and Air-Nitrogen Mixtures at Elevated Temperatures and Pressures," *Combust. Flame*, **10**, 95 (1966).
Crescitelli, S., G. Russo, and V. Tufano, "The Influence of Different Diluents on the Flammability Limits of Ethylene at High Temperatures and Pressures," *J. Hazard. Mater.*, **3**, 167 (1979).
Cutler, D. P., "The Ignition of Gases by Rapidly Heated Surfaces," *Combust. Flame*, **22**, 105 (1974).
Detz, C. M., "Threshold Conditions for the Ignition of Acetylene Gas by a Heated Wire," *Combust. Flame*, **26**, 45 (1976).
Fiumara, A., and P. Cardillo, "Influenza della Temperatura e della Pressione Sull'infiammabilita Dell'etilene," *Riv. Combust.*, **30**(9–10), 296 (1976).
Fox, R. O., "Computational Methods for Turbulent Reacting Flows in the Chemical Process Industry," *Rev. Inst. Fr. Pet.*, **51**(2), 215 (1996).
Frank-Kamenetskii, D. A., *The Theory of Thermal Explosion, Diffusion and Heat Transfer in Chemical Kinetics*, 2nd ed., Plenum Press, London (1969).
Gatica, J. E., J. Puszynski, and J. Hlavacek, "Reaction Front Propagation in Non Adiabatic Exothermic Reaction Flow Systems," *AIChE J.*, **33**(5), 819 (1987).
Gaube, J., H. Grosse-Wortmann, and K. H. Simmrock, "Explosionsgrenzen der Systeme $C_2H_4/O_2/N_2$ bis 26 at und 300°C sowie $C_2H_4/H_2/O_2/N_2$ bei 1 at und 20°C," *Chem. Ing. Tech.*, **40**, 660 (1968).
Gray, P., and P. R. Lee, "Thermal Explosion Theory," *Oxid. Combust. Rev.*, **2**, 1 (1967).
Hashiguchi, Y., T. Ogahara, M. Iwasaka, and K. Ozawa, "Effect of Pressure on the Detonation Limit of Ethylene," *Int. Chem. Eng.* **6**(4), 737 (1966).
Hilpert, R., "Wärmeabgabe von geheizten Drahten und Rohren im Luftstrom," *Forschung*, **4**(5), 215 (1933).
Hinze, J. O., *Turbulence*, 2nd ed., McGraw-Hill, New York (1975).
Hustad, J. E., and O. K. Sønju, "Experimental Studies of Lower Flammability Limits of Gases and Mixtures of Gases at Elevated Temperatures," *Combust. Flame*, **71**, 283 (1988).
Jones, W. P., and B. E. Launder, "The Prediction of Laminarization with a Two-Equation Model of Turbulence," *Int. J. Heat Mass Transfer*, **15**, 301 (1972).
Laurendeau, N. M., and R. N. Caron, "Influence of Hot Surface Size on Methane-Air Ignition Temperature," *Combust. Flame*, **46**, 213 (1982).
Leuckel, W., W. Nastoll, and N. Zarzalis, "Influence of Turbulence on Transient Premixed Flame Propagation Inside Closed Vessels," *Chem. Eng. Tech.*, **12**, 226 (1989).
Lewis, B., and G. Von Elbe, *Combustion, Flames, and Explosions of Gases*, Academic Press, New York (1961).
Libby, P. A., and F. A. Williams, *Turbulent Reacting Flows*, Academic Press, New York (1994).
Lovachev, L. A., V. S. Babkin, V. A. Bunev, A. V. V'Yun, V. N. Krivulin, and A. N. Baratov, "Flammability Limits: An Invited Review," *Combust. Flame*, **20**, 259 (1973).
Merzhanov, A. G., and A. E. Averson, "The Present State of the

Thermal Ignition Theory: An Invited Review,'' *Combust. Flame*, **16**, 89 (1971).
Miller, S. A., *Ethylene and Its Industrial Derivatives*, Ernest Benn, London (1969).
Nieuwstadt, F. T. M., *Turbulentie, Inleiding in de Theorie en Toepassingen van Turbulente Stroming*, Epsilon, Utrecht, The Netherlands (1992).
Oran, E. S., and J. P. Boris, ''Detailed Modelling of Combustion Systems,'' *Prog. Energy Combust. Sci.*, **7**, 1 (1981).
Perry, R. H., D. W. Green, and J. O. Maloney, *Perry's Chemical Engineers Handbook*, 6th ed., McGraw-Hill, New York (1984).
Raymond, L. R., and N. R. Amundson, ''Some Observations on Tubular Reactor Stability,'' *Can. J. Chem. Eng.*, 173 (1964).
Rodi, W., ''Turbulence Models and Their Application in Hydraulics —A State of the Art Review,'' Section on Fundamentals of Division II: Experimental and Mathematical Fluid Dynamics (1980).
Rota, R., P. Canu, S. Carra, and M. Morbidelli, ''Vented Gas Deflagration Modelling: A Simplified Approach,'' *Combust. Flame*, **85**, 319 (1991).
Schlichting, H., *Boundary Layer Theory*, 6th ed., McGraw-Hill, New York (1968).
Semenoff, N., ''Zur Theorie des Verbrennungsprozesses,'' *Z. Phys.*, **48**, 571 (1928).
Siccama, N. B., and K. R. Westerterp, ''The Explosion Region Becomes Smaller under Flow Conditions: The Ignition of Ethene-Air Mixtures with a Hot Surface,'' *Ind. Eng. Chem. Res.*, **32**, 1304 (1993).
Siccama, N. B., and K. R. Westerterp, ''Modelling of the Ignition of Ethene-Air Mixtures with a Hot Surface Under Flow Conditions,'' *Ind. Eng. Chem. Res.*, **34**, 1755 (1995).
Singh, D. J., and C. J. Jachimowski, ''Quasi Global Reaction Model for Ethylene Combustion,'' *AIAA J.*, **32**(1), 213 (1994).
Tenneckes, H., and J. L. Lumley, *A First Course in Turbulence*, MIT Press, Cambridge, MA (1972).
Ullmann, *Encyklopädie der technischen Chemie*, Vol. 20, Verlag Chemie, Weinheim, Germany, p. 4 (1981).
Ulsamer, J., ''Die Wärmeabgabe eines Drahtes oder Rohres an einen senkrecht zur Achse strömenden Gas-oder Flüssigkeitstrom,'' *Forschung*, **3**(2), 94 (1932).
Veser, G., and L. D. Schmidt, ''Ignition and Extinction in the Catalytic Oxidation of Hydrocarbons over Platinum,'' *AIChE J.*, **42**(4), 1077 (1996).
Warnatz, J., D. L. Baulch, C. J. Cobos, P. Frank, G. Hayman, Th. Just, J. A. Kerr, T. Murrells, M. J. Pilling, J. Troe, and R. W. Walker, ''Summary Table of Evaluated Kinetic Data for Combustion Modelling: Supplement 1,'' *Combust. Flame*, **98**, 59 (1994).
Watanabe, F., M. Mitsuhata, and T. Kumazawa, ''Process for Production of Ethylene Oxide,'' U.S. Patent No. 4,376,209 (1983).
Westbrook, C. K., and F. L. Dryer, ''Simplified Reaction Mechanisms for the Oxidation of Hydrocarbon Fuels in Flames,'' *Comb. Sci. Tech.*, **27**, 31 (1981).
Westbrook, C. K., F. L. Dryer, and K. P. Schug, ''Numerical Modelling of Ethylene Oxidation in Laminar Flames,'' *Combust. Flame*, **52**, 299 (1983).
White, A. G., ''Limits for the Propagation of Flame in Inflammable Gas-Air Mixtures. Part III. The Effect of Temperature on the Limits,'' *J. Chem. Soc.*, **127**, 672 (1925).
Wilhelm, R. H., ''Progress Towards the a Priori Design of Chemical Reactors,'' *Pure Appl. Chem.*, **5**(3–4), 403 (1962).
Williams, W. R., M. T. Stenzel, X. Song, and L. D. Schmidt, ''Bifurcation Behaviour of Homogeneous-Heterogeneous Combustion. I: Experimental Results over Platinum,'' *Combust. Flame*, **84**, 265 (1991).
Zabetakis, M. G., ''Flammability Characteristics of Combustible Gases and Vapours,'' PhD Thesis, Dept. of the Interior, Bureau of Mines, Washington, DC (1965).

Manuscript received Dec. 1, 1997, and revision received Oct. 22, 1998.